# Application of Non-Dispersive Infrared (NDIR) Spectroscopy to the Measurement of Atmospheric Trace Gases

A thesis presented in partial

fulfilment for the degree of

**Master of Science in Environmental Science**

at the

University of Canterbury,

Christchurch, New Zealand.


by

Louise Helen Crawley

2008

# Abstract

Gaseous pollutants have been an environmental concern since 1956, when the first clean air act was established in the United Kingdom. Monitoring of gaseous emissions is a legal requirement in most countries, and this has generated a large demand for inexpensive, portable, and versatile gas analysers for the measurement of gaseous emissions. Many of the current commercial gas analysers have differing advantages and disadvantages, however, high cost is an important factor. Instruments with low detection limits and the ability to measure multiple gases tend to be very expensive, whereas, single gas analysers tend to be much more affordable.

A non-dispersive infrared (NDIR) spectrometer, originally developed for a previous M.Sc. project, has been further developed in order to increase the sensitivity and to extend the instrument to the measurement of multiple gases. This type of instrument would be useful for environmental, industrial, and research applications. The instrument was inexpensive to construct when compared with the cost of current commercial gas analysers, is robust, and is partially portable around the laboratory.

Infrared radiation from two infrared sources, pass through adjacent sample and reference cells and into corresponding detector cells. A sample comprising the analyte gas is contained in the sample cell, a non-absorbing gas, such as argon, is contained in the reference cell, and pure analyte gas of interest is contained in the detector cells. The two identical detector cells, which follow the reference and sample cells in the infrared optic paths, communicate only through a differential capacitance manometer which accurately measures small pressure differences between the otherwise identical cells. Any trace amount of the analyte gas in the sample cell absorbs radiation, depleting the appropriate infrared frequencies. This results in lower energy incident on the sample detector cell, reducing the infrared induced pressure rise in that detector cell compared to the reference side detector cell. The pressure difference is

proportional to the concentration of absorbing gas in the sample cell, which is then determined using a calibration graph.

Carbon dioxide, methane, and nitrous oxide calibration graphs from 40 *ppm* to 1000 *ppm* have been successfully established, and detection limits of 10.33 *ppm* for $CO_2$, 8.81 *ppm* for $N_2O$ and 9.17 *ppm* for $CH_4$ were determined. Dried air samples measured using the spectrometer gave an average value of 382 ± 9.6 *ppm* which can be compared to the latest global atmospheric loading of 382.4 *ppm*.

# Acknowledgements

I would like to dedicate this thesis to leaks. Not the vegetable (leek), but the problem I spent most of my research trying to fix! You might have won the battles, but I won the war!

I would firstly like to thank my supervisor, Professor Peter Harland, for providing me with this research opportunity, advice, encouragement, and support over the past two years. I have learnt a great deal from him and have enjoyed the many good stories he has to tell.

I would like to thank the mechanical, electrical and glassblowing technical staff, because if it wasn't for them the instrument would have big holes in it! I would especially like to thank Danny Leonard, Wayne Mackay, Rob McGregor and Steven Graham for putting up with my inarticulate questions and my constant demands!

Thanks to my parents, Lynne and Trevor, for their overwhelming support throughout my whole university career, but especially during the completion of my masters degree. I would like to thank my dad for his financial support, I especially appreciate living rent free for the past five years! And my mum for providing me with a relaxing place to visit when the going's got rough, and I needed to escape!

I would like to put a big thank you to all my friends in the department for their friendship, support, and, for many (you know who you are!!), making me laugh when it was needed. It was nice to have you guys around, especially during those long six month stints when I was overwhelmed with leaks!!!

And last, but defiantly not least, I would like to thank my partner Matthew for his love, support, and for generally putting up with my sometimes incoherent behaviour. You have been a great friend and partner, and I couldn't have done it without you!

# Table of Contents

# List of Figures

# List of Tables

## Chapter I

# Introduction

Gaseous pollutants released into the atmosphere are an environmental concern both on a global scale, for example climate change, and a local scale, for example photochemical smog. Current methods for measuring and monitoring gases are costly and limited in their applications. The main objective of this research was to develop a gas analyser with high sensitivity, high versatility and a low associated cost.

Many of the commercially available gas measurement techniques with high sensitivity and versatility are also very expensive. There is a small selection of commercially available instruments that are affordable and also achieve high sensitivity, however, these instruments are typically single gas analysers and are limited in theire application. This research was focused on the development of a non-dispersive infrared (NDIR) spectrometer initially constructed by Timothy Simpson as an M.Sc. research project in 2004. The goal was to achieve high sensitivity for trace gas measurements of specific environmental gases, while being of low cost compared to currently available commercial instruments. Carbon dioxide ($CO_2$), nitrous oxide ($N_2O$) and methane ($CH_4$) gases were selected as analyte gases because they are all known greenhouse gases arising from intensive farming.

The instrument is based on non-dispersive infrared absorption spectroscopy. NDIR analysers have been used for environmental, industrial and research applications.

NDIR instruments are typically a simple design and can be built with inexpensive components.

This thesis begins with an introduction to infrared analysis in chapter 2, followed by a description of the operation of non-dispersive infrared analysers in chapter 3. A case study on environmental gas measurement is presented in chapter 4, as this is a possible application for this type of instrument. The instrument developed by Simpson and the initial modifications made in the first few months of this project are discussed in chapter 5. Chapter 6 discusses instrument developments carried out later in the project in order to improve sensitivity. Chapter 7 presents the data collected using the instrument. This includes determination of the sensitivity, and response of the instrument for three greenhouse gases, carbon dioxide, nitrous oxide, and methane. The final chapter is a conclusion and recommendations for future developments.

# Chapter II

# Infrared Spectroscopy and Analysis

## 2.1 Introduction

Infrared spectroscopy is a very important tool used for a range of qualitative and quantitative applications. This technique is commonly used for medical and environmental applications such as breath analysis and the measurement of trace atmospheric constituents, respectively. In addition, characterisation of chemical compounds in research and analytical laboratories can be performed with infrared spectroscopy.

The infrared region in the electromagnetic spectrum ranges from 12,500 $cm^{-1}$ to 100 $cm^{-1}$. This region is divided into three sub-regions (near-, mid- and far-infrared) which require different instrumentation and have different uses. The near-IR region ranges from 12,500 $cm^{-1}$ to 4,000 $cm^{-1}$ and is commonly used for industrial applications. The far-IR region ranges from 600 $cm^{-1}$ to 100 $cm^{-1}$ and is usually used for research and academic applications. The mid-IR region is the most important region and ranges from 4,000 $cm^{-1}$ to 600 $cm^{-1}$. Most infrared active molecules absorb in the mid-IR region where the photon energy corresponds to their fundamental molecular absorption bands. This region is used for both quantitative and qualitative analysis.

Infrared analysis is particularly useful as it can be used for analysis of all three physical states, solid, liquid and gas and, with the exception of a few gas phase species with zero dipole moment, it is applicable to all molecules giving a "fingerprint" spectrum (see below).

## 2.2 Infrared Analysis

Infrared spectroscopy is commonly used for chemical analysis due to the ability of infrared radiation to interact with a large variety of molecules. When infrared radiation passes through an infrared active sample some of the radiation is absorbed decreasing the intensity of the resulting radiation.

For a molecule to be infrared active, a change in dipole moment (**μ**) of the molecule must occur. An electric dipole occurs when two adjacent atoms within a molecule have different electronegativities or charges, q and –q, separated by a distance **r** and is represented by a vector **μ**. The dipole moment is defined as the product of the charge q and the vector separation **r**. A change in dipole moment occurs when the distance between the two atoms forming the dipole changes due to vibration or rotation in the molecule.

If the dipole moment changes with internal motion this gives rise to an oscillating electric field. Electromagnetic radiation with its electric vector oscillating at the same frequency can interact and be absorbed by the molecule, resulting in a change in the energy level and increasing the vibrational and/or rotational quantum number.

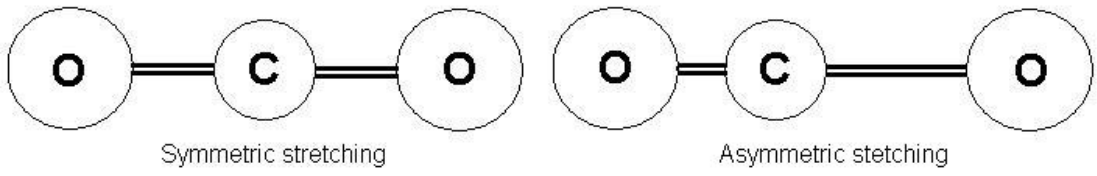


**Figure 2.1**: Symmetric and asymmetric stretching of carbon dioxide.

Taking $CO_2$ as an example, if the molecule undergoes symmetric vibration the change in the electric dipole of the C=O bonds is the same but in opposite directions. The end

result is that there is no net change in the overall dipole moment of the molecule and symmetric stretching does not result in the absorption of infrared radiation and is termed infrared inactive. In contrast, asymmetric stretching, where one of the C=O bonds stretches as the other compresses, does result in an overall change in the dipole moment of the molecule and this vibrational mode is infrared active (same with bending).

Atomic species and homonuclear diatomics do not meet the criteria for infrared active molecules. Atomic species, such as Ar, contain only one atom and therefore cannot exhibit a dipole or a dipole moment. Homonuclear diatomics, such as $O_2$ and $N_2$, have adjacent atoms with identical electronegativities, and therefore vibration and rotation does not result in a change in dipole moment.

### 2.2.1 Qualitative Analysis

Qualitative analysis is used for the characterisation of a compound by comparing its infrared spectrum with a spectral library of known substances. Measured in the mid-IR region, the infrared spectrometer measures the absorption at various wavelengths due to the vibrations (rotation-vibration at high resolution) of different functional groups in the molecule. This gives rise to a fingerprint spectrum; that is, no two molecules exhibit exactly the same spectrum.

### 2.2.2 Quantitative Analysis

Quantitative analysis is used for measuring the quantity or concentration of a substance and is achieved using Beer-Lamberts law [Atkins 2006]. Because molecules absorb infrared radiation in bands specific to the molecule, comparing incident and resulting radiation at those specific wavelengths allows quantification of the sample concentration.

$$A_\lambda = \log_{10} \frac{I_{o,\lambda}}{I_\lambda} \qquad 2.1$$

Where $A_\lambda$ = Absorbance of the sample at wavelength λ.

$I_{0\lambda}$ = Intensity of the incident radiation on the sample at wavelength λ.

$I_{\lambda}$ = Intensity of radiation exiting from the sample at wavelength λ.

The Beer-Lamberts law expresses absorption of radiation as a linear relationship with the sample concentration at a fixed wavelength.

$$A_{\lambda} = \varepsilon_{\lambda} c l \qquad 2.2$$

Where $\varepsilon_{\lambda}$ = Extinction coefficient of the sample at wavelength λ ($L\ mol^{-1}\ cm^{-1}$).

$c$ = Concentration of the sample ($mol\ L^{-1}$).

$l$ = Path length of the sample ($cm$).

If the path length of the sample and the wavelength are kept constant, a calibration graph of absorbance versus concentration can be produced. The calibration graph can then be used to determine the unknown concentration in a sample [Simpson 2004].

## 2.3 Infrared Spectrometer Components

There are a wide range of different infrared spectrometers depending on their use and infrared region of interest. However, they all have the same basic components: infrared source; a detector; and an optical system. Dispersive instruments also require a grating. Sources, detectors and other components used in infrared spectrometers are discussed in the sections below.

### 2.3.1 Infrared Sources

Infrared sources are made from various solid materials which when heated release energy similar to that of a black body radiator. The power output from these sources closely follows the Planck distribution [Atkins 2006]:

$$\rho = \frac{8\pi hc}{\lambda^5 (e^{hc/\lambda kT} - 1)} \qquad 2.3$$

Where $\rho$ = Absorbance of the sample ($W\,m^{-2}$)

$c$ = Speed of light ($2.997 \times 10^{8}\ m\,s^{-1}$)

$h$ = Planck's constant ($6.626 \times 10^{-34}\ J\,s$)

$\lambda$ = Wavelength ($m$)

$k$ = Boltzman constant ($1.381 \times 10^{-23}\ J\,K^{-1}$)

$T$ = Temperature ($K$)

The following image illustrates the energy distribution of a black body radiator at various temperatures.

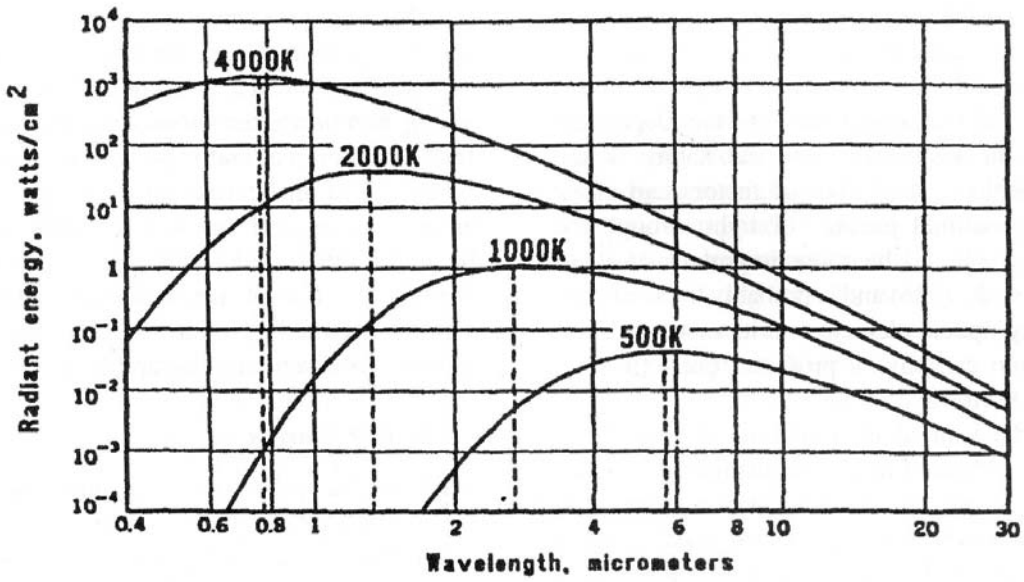


**Figure 2.2**: Distribution of energy for a black body radiator [Cazes 2005].

Figure 2.1 illustrates the emission profile for a typical black body radiator at varying temperatures. The figure shows that a reasonable operating temperature is between 1000 $K$ and 1500 $K$ for emission in the mid-IR region (2.5 to 14 $\mu m$). Temperatures above this range result in a large increase of radiation in the visible region of the spectrum, but do not significantly increase the mid-IR radiation.

There are numerous different infrared sources that have been used, or are in use in current infrared spectrometers. The majority of these sources release radiation over

the entire infrared region, while others release radiation at specific single wavelengths. These sources are detailed below.

**Lasers**

A laser is *L*ight *A*mplification by *S*timulated *E*mission of *R*adiation. Traditional diode lasers are interband semiconductors in which light emission occurs from electron-hole recombination [Heard 2006].

Diode lasers currently available for detection of gases in the near-IR are typically made of group thirteen and fifteen elements, for example GaAs/AlGaAs and InGaAs/InP [Amato 2002]. Lead salt diode lasers are the main lasers commercially available for measurement in the mid-IR region. The main advantage of a near-IR laser is its ability to operate at room temperature, in contrast to mid-IR lasers which require cryogenic cooling. The laser frequency of diode lasers can also be continuously and selectively tuned by changing the injection current and the temperature. This allows specific wavelengths to be obtained. The main disadvantage for applications in the near-IR is the low intensity molecular line strength that occurs resulting in low sensitivity. However, this can be overcome by increasing the optical path length with use of various optical mirrors and cells [Amato 2002] [Gagliardi 2002]. These are discussed later in this chapter.

**Globar**

The Globar is a robust infrared source made of a silicon carbide rod which operates at high temperatures, typically between 1,200 °C and 2,000 °*C*. The Globar is electrically heated and gives a relatively high power output. However, a disadvantage of the Globar is the large amount of heat that is transferred through the instrument due to the high power output. Cooling of the electrodes, where a large proportion of the power is dissipated, is a necessity [Ewing 1997].

#### Nernst Glower

The Nernst Glower is composed of rare earth metal oxides, such as zirconium and yttrium [Ewing 1997] and similar to the Globar it has high operating temperatures up to 2,000 °*C*. The Nernst Glower is relatively inexpensive and is self sustaining at high temperatures. Disadvantages include the requirement for preheating before use and its relativity short lifetime of approximately ten months [Simpson 2004].

#### Heated Ceramic Rod – Opperman

The Opperman is a specific type of heated ceramic infrared source. A nichrome or platinum wire, that is electrically heated, is located in the centre of a ceramic rod containing a mixture of earth metal oxides. The wire heats the mixture of metal oxides which in turn heats the ceramic rod releasing radiation [Ewing 1997]. The Opperman generally has a short lifetime and is not used in commercial infrared spectrometers [Simpson 2004].

#### Nichrome Wire

Nichrome wire is used as the infrared source in this project. The electrically heated source operates at lower temperatures than both the Nernst Glower and the Globar, generally between 1,000 °C and 1,100 °*C*. The main disadvantage to the nichrome wire is oxidation of the filament and thermal stressing that can occur over long periods of time [Ewing 1997].

### 2.3.2 Infrared Detectors

Detectors used in commercial infrared spectrometers vary depending on their sensitivity and performance. These detectors range from simple thermocouples to more complicated pyroelectric detectors, and are discussed below.

### Thermocouple

A thermocouple is made from two dissimilar metals; a common combination includes bismuth and antimony [Ewing 1997] [Willard 1988]. The detector response is proportional to the temperature over the junction between the two metals, which is dependant on the intensity of the incident radiation. Disadvantages to using a thermocouple as a detector includes a slow response time and low sensitivity, however, the sensitivity can be increased by thermal isolation of the junction [Ewing 1997].

### Thermopile

A thermopile is a group of thermocouples connected together which develop a potential difference over the dissimilar metal junctions when their temperatures differ. The temperature differences result from infrared radiation absorbing by an absorber material connected to the thermocouples. Thermopiles are a very common thermal detector used for infrared spectroscopy [Willard 1988].

### Bolometer

A bolometer is an infrared detector made from semiconductor material with a high temperature coefficient of resistivity. The electrical resistance changes with the bolometers interaction with infrared radiation, allowing the intensity of the radiation to be determined. Bolometers generally have low sensitivity and slow response time [Ewing 1997], however sensitivity of the bolometer increases as the size of the bolometer decreases [Simpson 2004].

### Luft Type Detector

The Luft type detector is used for this research project. The detector contains two gas cells filled with the analyte gas of interest and are separated by a capacitive diaphragm. One side of the detector is aligned with a cell that contains the sample analyte gas, and the other side of the detector is aligned with a cell containing an inert,

non-absorbing gas. Identical infrared beams are passed through each cell and into the detector where the diaphragm flexes from differences in absorption between the two sides of the detector cell. This deflection produces a voltage which is proportional to the concentration of analyte gas in the sample cell. A disadvantage to this type of detector is that it is sensitive to mechanical vibration [Simpson 2004]. The luft type detector will be further discussed in chapter 5.

#### Pyroelectric Detectors

A pyroelectric detector is made from a pyroelectric material, such as triglycine sulfate. Triglycine sulfate is commonly found in pyroelectric detectors used for infrared spectroscopy. The material is connected to two electrodes which produce a signal that is dependent on the change in temperature of the detecting material [Ewing 1997]. In order to use this type of detector the infrared radiation must be modulated at audio frequencies using a Michelson interferometer (as used in Fourier transform infrared instruments).

#### Photo-conductive Detectors

A common material used for photo-conductive detectors in infrared applications is PbSe [Mecca 2000] [Theocharous 2007]. The electrical conductance changes with incident infrared energy, similar to the bolometer. Advantages of photo-conductive detectors include high detection levels, fast response time and are reasonable affordable. Disadvantages of photo-conductive detectors include thermal drift and production of thermal noise [Mecca 2000].

### 2.3.3 Other Infrared Components

#### Monochromators and Interferometers

Monochromators and interferometers are used to filter the radiation of unwanted wavelengths. A monochromator uses mirrors or gratings to achieve wavelength selection. Interferometers are usually a transmitting material with two partially

reflecting layers. The distance between these layers determines the wavelength of transmitted light [Ewing 1997].

**Multi-pass Cells**

Multi-pass cells allow increased sensitivity due to an increase in the absorption path length. They contain a set of mirrors which reflect the optical beam back and forth resulting in an increase in path length.

The following diagram illustrates the three main types of multi-pass cell used for atmospheric gas analysis; Astigmatic Herriott cell, Herriott cell, and White cell.

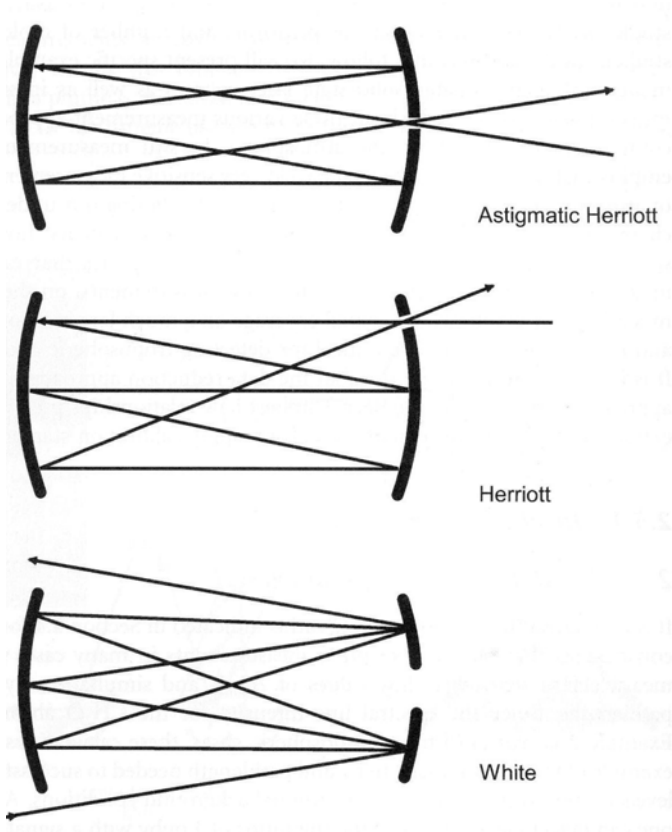


**Figure 2.3**: Diagram of an Astigmatic Herriott multi-pass cell, a Herriott multi-pass cell, and a White multi-pass cell [Heard 2006].

An Astigmatic Herriott multi-pass cell contains two mirrors. The radii of curvature of both mirrors are different in the horizontal and vertical planes [Heard 2006]. One

mirror contains a small hole in the centre of one of the mirrors which the incident and resulting optical beams both pass through.

A Herriott multi-pass cell contains two spherical mirrors spaced close to their common radii of curvatures. One mirror contains a small hole slightly off axis which the incident and resulting beams pass through.

A white multi-pass cell has three spherical mirrors with identical radii of curvature. The front mirror is placed at its confocal distance from the two identical 'D' shaped mirrors [Heard 2006]. The input beam is reflected off the first 'D' shaped mirror and recirculates between the three mirrors before exiting from reflection off the second D shaped mirror.

**Mirrors, Lenses and Collimators**

Collimators, mirrors and lenses are used in spectrometers to direct the beam of radiation on a specific path.

A collimator is simply a tube or slit in which the beam passes through. Collimators cannot be used for long path lengths because of losses in radiation due to divergence of the beam. Mirrors and lenses are used to focus the light and avoid divergence of the beam reducing the loss of radiation. As noted above, mirrors are used in multi-pass cells, however, lenses are also used in spectrometers to increase the path length. Mirrors and lenses are usually used in dispersive infrared spectrometers and are absent from non-dispersive infrared spectrometers.

**Sample Containment**

The containment of the sample will depend on whether it is a solid, liquid or gaseous phase sample. Solids are generally contained between two mull plates and placed in the radiation path length. The solid is in the form of a fine powder which has been made into a paste by addition of a mulling agent such as nujol [Willard 1988]. Liquids

are contained in small transmitting cuvettes with a standard path length of 1 cm. However, larger path lengths are required for dilute solutions.

Gases are contained in a cell sealed with infrared transmitting windows. Usually the path length is 10 *cm* [Willard 1988], however, when this is not satisfactory, multi-pass cells can be used. The windows used will depend on the gas being analysed as it must transmit at the wavelength at which the gas absorbs. The windows have a range of properties and associated costs. Windows used in gas analysis must be chosen carefully as the windows are often hygroscopic and are susceptible to fogging and degradation.

The following table illustrates a range of infrared transmitting materials used in commercial infrared spectrometers.

| Material | Wavelength range ($\mu m$) | Wavenumber ($cm^{-1}$) | Refractive index at 2 $\mu m$ |
|---|---|---|---|
| NaCl | 0.25 – 17 | 40,000 – 590 | 1.52 |
| KBr | 0.25 – 25 | 40,000 – 400 | 1.53 |
| KCl | 0.30 – 20 | 33,000 – 500 | 1.50 |
| $CaF_2$ (Irtran-3) | 0.15 – 9 | 66,700 – 1,110 | 1.40 |
| MgO (Irtran-5) | 0.39 – 9.4 | 25,600 – 1,060 | 1.71 |
| TlBr-TlI (KRS-5) | 0.50 – 35 | 20,000 – 286 | 2.37 |
| $SiO_2$ (quartz) | 0.16 – 3.7 | 26,500 – 2,700 | 1.46 |

**Table 2.1**: Transmittance of commonly used infrared transmitting materials [Willard 1988].
Note: the mid-infrared spans the wavelength range from 2.5 to 14 $\mu m$.

### Amplifiers and Beam Choppers

An amplifier is a device that is used to increase the amplitude of an electronic signal. The gain of the amplifier is given as the ratio of the output signal (voltage or current) to the input signal.

Operational amplifiers are used to perform a range of mathematical operations, from basic addition and subtraction to more complicated integration and differentiation on an electronic signal [Kalvoda 1975]. There are numerous types of operational amplifiers, including differential and lock-in. Differential and lock-in amplifiers are both used for signal recovery when the signal to noise ratio is low. A lock-in amplifier measures and amplifies the difference between a reference signal and an analytical signal of the same frequency [Ewing 1997]. This can be achieved using a beam modulator or chopper.

Beam modulators or choppers are usually rotating discs containing apertures which allow radiation to pass through [Skoog 1992]. The radiation is blocked and then unblocked as the solid disc and apertures alternate in front of the beam. The modulation frequency is determined from the speed of the rotating disc.

# Chapter III

# Non-dispersive Infrared (NDIR) Spectroscopy

## 3.1 Introduction

In this chapter non-dispersive infrared (NDIR) spectroscopy and some of its applications in the environment, industry and in research are discussed.

Infrared spectrometers can be divided into three categories: dispersive; multiplex; and non-dispersive. Dispersive instruments use gratings or prisms to achieve wavelength selection and are typically used for qualitative work. Multiplex instruments, or Fourier Transform Infrared (FTIR) Spectrometers, use a Michelson interferometer to modulate the intensity of the infrared radiation as a function of frequency, and then employ Fourier transform algorithms to convert the resulting time dependent spectrum into a standard wavenumber spectrum. FTIR spectroscopy can be used for both qualitative and quantitative work. Non-dispersive instruments have a much simpler design than both dispersive and multiplex instruments. This is because they do not use any gratings of prisms to achieve wavelength selection or employ the use of an interferometer and Fourier transforms. Non-dispersive instruments have been used for quantitative determination of a variety of gaseous species in the atmosphere by absorption, emission and reflectance spectroscopy [Skoog 1998]. Non-dispersive infrared spectrometers tend to be rugged, easy to maintain and operate, and are much less expensive than other infrared spectrometers.

## 3.2 Non-dispersive Infrared Analysers

Non-dispersive infrared spectrometers work by measuring the intensity of light absorbed by a sample. The instrument has three basic components, an infrared source; a sample cell containing the gas of interest; and a detector [Simpson 2004]. Most NDIR instruments use two infrared sources and the difference in intensity of the two is measured.

There are three main types of non-dispersive infrared spectrometers: Total absorption; negative filter; and positive filter. Total absorption analysers have no selectivity towards any gas and are based on total absorbance of infrared radiation. Negative filter analysers gain selectivity by removal of a specific spectral region. In contrast positive filter analysers gain selectivity by implementing a detector containing the infrared absorbing gas of interest.

### 3.2.1 Total Absorption

As illustrated in figure 3.1, total absorption analysers contain two infrared sources, a reference cell containing a non-absorbing gas, a sample cell containing a sample of gases to be measured, and a detector. Energy from each infrared source passes through the reference and sample cells to the detector. When the sample cell is evacuated or filled with an inert gas, the sample beam radiation reaching the detector is the same as the reference beam radiation. However, when the sample cell contains a sample, radiation is absorbed, reducing the radiation reaching the detector. The difference in signal received from the two beams is measured by the detector and is related to the amount of absorbing gas in the detector cell.

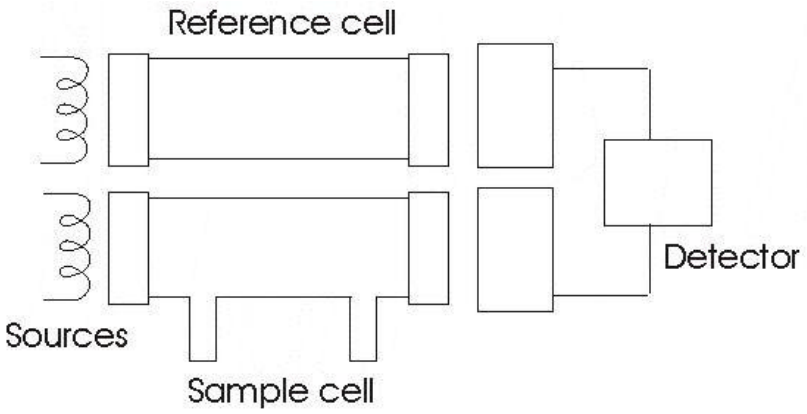


**Figure 3.1**: Total absorption non-dispersive infrared spectrometer.

Because total absorption contains no wavelength selectivity, total absorption may be used only when the infrared spectrum of the sample is unaffected by any other component in the cell.

### 3.2.2 Negative Filter

A negative filter NDIR instrument is illustrated in figure 3.2. It contains two infrared sources, a sample cell, a sensitising cell, a compensation cell, two filter cells, and two detectors. The sample continuously flows through the sample cell. Two beams from the infrared sources pass through the sample cell. One of the beams then passes through the compensation cell which contains a non-absorbing gas, while the other beam passes through the sensitising cell containing the infrared absorbing gas of interest. Both beams then reach two independent detectors which are bolometers electrically connected through a Wheatstone Bridge [Kendall 1966].

When the sample cell is empty, the radiation reaching each individual detector is not equal due to absorption of radiation in the sensitising cell. The radiation transmitted from the compensation side is therefore reduced so identical intensities of radiation are reaching each bolometer. When the gas of interest flows through the sample cell it diminishes the radiation on the compensation side from absorption by the gas. However, the radiation on the sensitising side is not reduced since the gas in the sensitising cell has already removed the energy at the wavelengths specific to the gas of interest. The radiation on the compensation side now has less energy than the

radiation on the sensitising side, a condition called positive sensitisation [Kendall 1966]

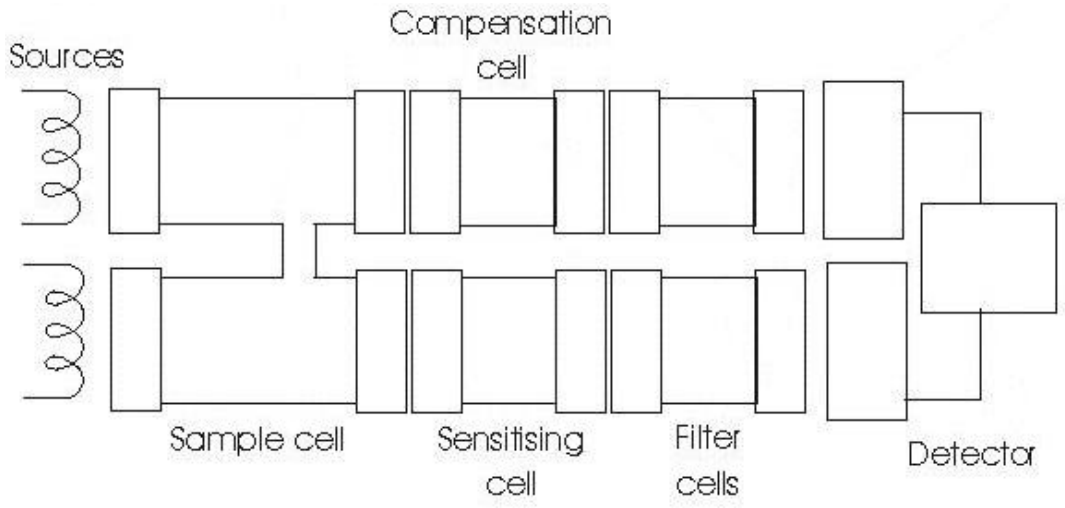


**Figure 3.2**: Negative filter non-dispersive infrared spectrometer.

Some gases have overlapping regions in the spectrum which can cause interference. An example of two gases with overlapping absorption bands are carbon dioxide and water. If one was to measure carbon dioxide in a sample, filter cells containing water vapour must be used to remove interference. The filter cells are placed on both reference and sample sides so the two optical paths are equally decreased by the radiation energy. As the radiation passes through the filter cell the water absorbs all of the radiation at its specific wavelengths. This results in only the difference in energy for the carbon dioxide being measured.

### 3.3.3 Positive Filter

Figure 3.3 illustrates a positive filter NDIR spectrometer. It includes two infrared sources, a reference cell containing a non-absorbing gas, a sample cell which the sample flows through, and a detector. Wavelength selection is achieved through selectivity in the detector. The detector, a luft type, contains two gas cells filled with an infrared absorbing gas and separated by a thin metal diaphragm. Selectivity is gained because absorption of gas in the detector occurs only at wavelengths which correspond to the spectrum of that gas [Kendall 1966].

Radiation released from the sources is transmitted through the reference and sample cells and into corresponding sides of the detector. When the sample cell is empty the radiation reaching each side of the detector is equal, resulting in identical pressures due to equal absorption of the radiation. However, when a sample flows through the sample cell, infrared radiation is absorbed reducing the radiation incident on the sample side of the detector. This results in a pressure difference between the two sides of the detector. The pressure difference causes the diaphragm to flex, changing the capacitance between the diaphragm and an adjacent stationary electrode (differential capacitance manometer). The resulting voltage output is proportional to the pressure difference in the detector and the concentration of gas in the sample cell.

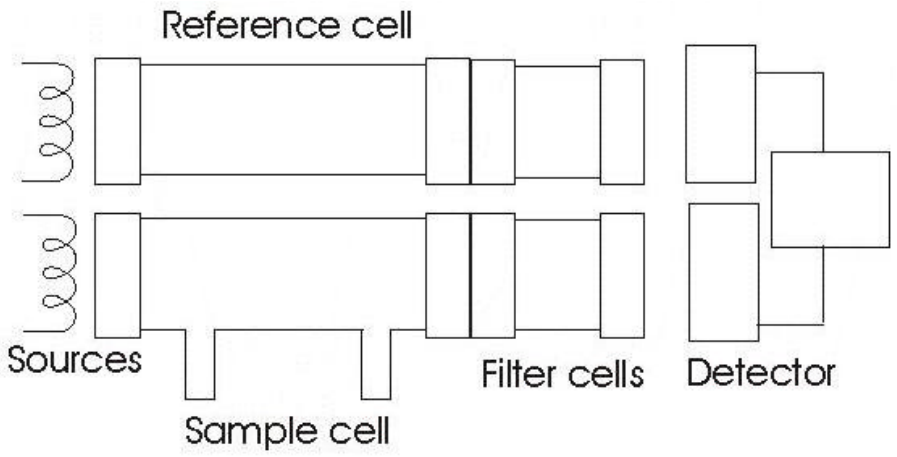


**Figure 3.3**: Positive filter non-dispersive infrared spectrometer.

## 3.3 Applications of Non-dispersive Infrared Spectroscopy

Over the years there have been numerous uses of non-dispersive infrared spectroscopy for environmental, industrial and research applications. Non-dispersive infrared spectroscopy was found to be a good alternative to other gas analysis techniques. This is due to its relatively low cost, ease of use and simple design. So, the development of an NDIR spectrometer for a specific purpose is a viable option. Selections of applications are discussed below.

### 3.3.1 Environmental Applications

Environmental applications include monitoring of emissions from vehicles, industrial sites and the measurement of other trace atmospheric gases.

#### Vehicle Gas Emission Monitoring

Vehicles emit a range of pollutants into the atmosphere including carbon dioxide, carbon monoxide, nitrogen oxides, volatile organic compounds (VOC) and poly-aromatic hydrocarbons (PAH's). These pollutants are harmful to human health and local flora and fauna. Nitrogen oxides emitted from vehicles are responsible for the production of photochemical smog in many major cities around the world.

The application of the EU-Directive 92/55/EEC in Spain forces owners to submit their vehicles for routine tests (the Technical Inspection of Vehicles, ITV) to check gas emissions [de Castro 1999]. Carbon dioxide and carbon monoxide are monitored using non-dispersive infrared spectroscopy; however other pollutants such as hydrocarbons and nitrogen oxides are measured using a flame ionisation detector and a chemiluminescent analyser, respectively.

The University of Denver has conducted research into traffic emissions monitoring. This research has lead to the development of a non-dispersive infrared spectrometer to measure carbon monoxide exhaust emissions in traffic flows in order to pinpoint large polluting vehicles. The Fuel Efficiency Automobile Test (FEAT) [de Castro 1999] measures the carbon monoxide to carbon dioxide ratios in the exhaust of passing vehicles. This is achieved from an infrared beam which is transmitted across the road and through which vehicles pass.

#### Inorganic Carbon in Oceans

The earth's oceans are the major sink for atmospheric carbon dioxide, and long-term fluxes of carbon dioxide between the oceans and the atmosphere may have an astounding effect on the climate. For this reason, analytical techniques with high

accuracy and precision need to be developed for the determination of the carbon dioxide dissolved in our oceans.

The current and most commonly used method for determining total inorganic carbon ($C_T$) in sea water is through the use of coulometric detection which has a slow response time (fifteen minutes per sample), and uses hazardous chemicals. Two non-dispersive infrared spectroscopy methods have been developed for the determination of $C_T$ in sea water.

The first method is based on continuous gas extraction of carbon dioxide from acidified seawater that is pumped through an extraction cell at a constant flow rate. The extracted carbon dioxide is then measured using non-dispersive infrared spectroscopy. Compared to the coulometric method, the NDIR method is fast (five minutes per sample), requires small sample volumes (less than 50 $mL$), and does not use any hazardous chemicals [Katin 2005].

The second method is similar to the method above, however, the system uses a gas-permeable hydrophobic membrane contractor to help remove carbon dioxide from the acidified sea water [Bandstra 2006]. Once the carbon dioxide is stripped from the membrane contractor it is measured using non-dispersive infrared spectroscopy. The system can resolve total carbon dioxide concentrations with accuracy and precision of better than ± 0.1% and has a response time of six seconds [Bandstra 2006]. This method is easy to set up and is the fastest of the three methods.

### 3.3.2 Industrial Applications – Nuclear Fuels

One of the most important quantities that specify the physico-chemico state of a uranium-plutonium mixed oxide (MOX) fuel pallet is the oxygen-to-metal atomic ratio (O/M ratio) [Hiyama 1999]. Thermogravimetric methods, solid-electrode based coulometric techniques, and x-ray determination have all been used for the determination of the O/M ratio. These tests require complex operations that are extremely time consuming, which means they are unsuitable for use as a quality assurance test in a fuel pallet fabrication plant.

The use of non-dispersive infrared spectroscopy following the generation of carbon monoxide allows this ratio to be determined. A sample is introduced into molten metal in a graphite crucible and the oxygen is released as carbon monoxide following equation 3.1 below.

$$M_xO_y(solid) + yC(solid) \rightarrow yCO(gas) + xM(liquid) \qquad 3.1$$

The carbon monoxide evolved is diluted by the gas dilution unit, and then measured using non-dispersive infrared spectroscopy [Hiyama 1999]. It is a simple and fast technique which gave good agreement when compared to the gravimetric methods.

### 3.3.3 Research Applications – Composition of Cigarette Smoke

Cigarette smoke contains both gases and particulates containing thousands of constituents. For research into the combustion of cigarettes, a quantitative method and sampling system must be developed that will measure the constituents in the smoke without altering any properties or interfere with the combustion. A four Quantum Cascade laser spectrometer with dual gas sampling cells has been developed [Baren 2004] which meets these requirements.

The developed spectrometer has the ability to measure seven constituents in cigarette smoke simultaneously [Baren 2004]. A non-dispersive infrared analyser is used to provide a reference for which the accuracy of the spectrometer results can be determined. This is achieved by comparing simultaneous measurements of carbon dioxide by the developed spectrometer with the non-dispersive infrared analyser. The non-dispersive infrared analyser detected carbon dioxide in the sidestream cigarette smoke at approximately 800 *ppmv* while the carbon dioxide in mainstream cigarette smoke measurements were in the 10,000 to 20,000 *ppmv* range [Baren 2004].*

*MS smoke is released from the butt of the cigarette, while SS smoke is released form the lit end.

# Chapter IV

# Case Study: Environmental Gas Measurement

## 4.1 Introduction

The measurement of gaseous pollutants released into the atmosphere is now a legal requirement in most countries. There is a long list of known pollutants which can affect human health, the welfare of local flora and fauna, and many which are associated with climate change.

There is a wide range of analytical instruments on the market today specifically for the measurement of trace gases. These instruments vary in expense, advantages, and limitations as an analytical instrument. A selection of these instruments and gaseous pollutants are discussed in this chapter.

## 4.2 Background of Environmental Gas Monitoring

A reduction in air quality has been noted since the industrial revolution; however, it wasn't until 1952 in Britain when air quality became a major concern. In 1952 a Winter smog in London took the lives of approximately 4000 citizens due to particulate pollution and sulphur dioxide from coal combustion [O'Neill 1998]. These deaths led to the development of the clean air acts of 1956 and 1968 [Cambell 1997].

Also in the 1950's, in the United States, California had an increase in the use of motor vehicles which resulted in an increase in concentrations of nitrogen oxides and unburned hydrocarbons. Increases in nitrogen oxides resulted in the formation of the notable Los Angeles photochemical smog [Cambell 1997].

Over the years many countries all over the world have developed air quality legislation to protect the health of the citizens and the environment. Severe and uncontrolled air pollution can cause serious health and economic problems. Health problems include irritation and reduction in respiratory function from particulate material and many common gaseous pollutants [Bernstein 2008]. Economic problems can arise from damage to historical buildings and monuments due to acid rain, from the emission of sulphur dioxide during the combustion of sulphur containing coals.

Many countries have developed ambient air quality standards for specific gases and particulates. Monitoring sites across a local area are used to monitor for gases and particulates to ensure exposure to certain pollutants by the local community are within these standards. In the United States, the Environmental Protection Agency (EPA) has a set of national air quality standards which each state must meet in order to achieve compliance. Tables 4.1 and 4.2 show the ambient air quality standards for New Zealand and United States, respectively.

| **Pollutant** | **Standard** | | **Description** |
|---|---|---|---|
| Carbon monoxide (CO) | 10 $mg/m^3$ | 8-hour mean | Not to be exceeded more than once per year. |
| Nitrogen dioxide ($NO_2$) | 200 $\mu g/m^3$ | 1-hour mean | Not to be exceeded more than nine times per year. |
| Ozone ($O_3$) | 150 $\mu g/m^3$ | 1-hour mean | Never to be exceeded. |
| Sulphur dioxide ($SO_2$) | 350 $\mu g/m^3$ | 1-hour mean | Not to be exceeded more than nine times per year. |
| | 570 $\mu g/m^3$ | 1-hour mean | Never to be exceeded. |

**Table 4.1**: Ambient air quality standards, New Zealand[1].

[1] Ministry for the environment, New Zealand. www.mfe.govt.nz

| Pollutant | Standard | | Description |
|---|---|---|---|
| Carbon monoxide (CO) | 10 $mg/m^3$ | 8-hour mean | Not to be exceeded more than once per year. |
| | 40 $mg/m^3$ | 1-hour mean | Not to be exceeded more than once per year. |
| Nitrogen dioxide ($NO_2$) | 100 $\mu g/m^3$ | Annual | |
| Ozone ($O_3$) | 0.075 ppm | 8-hour mean | The 3-year average of the fourth-highest daily maximum 8-hour average ozone concentration over each year must not exceed 0.075 ppm. |
| Sulphur dioxide ($SO_2$) | 0.03 ppm | Annual | |
| | 0.14 ppm | 24-hour | Not to be exceeded more than once per year. |

**Table 4.2**: Ambient air quality standards, United States[2].

Countries also issue legislation and guidelines for industrial companies which discharge pollutants into the atmosphere. As a result, monitoring of gaseous emissions from an industrial plant is now a legal requirement in these countries in order to achieve national or local compliance.

In the United Kingdom, the Environment Agency issues guidelines for emissions of pollutants from industrial plants, any monitoring requirements, and pollutant removal technology that must be used. The industrial plant must undertake emissions monitoring at its own expense and report the results to the Environment Agency to demonstrate compliance [Clarke 1997]. The Environmental Protection Agency (EPA), in the United States, also issues guidelines for emissions from industrial plants, yet also allows emission trading between plants in relatively pollution free areas. The increase in emissions at one plant is allowed if there is an equal reduction in emissions at another. The building of a new plant is only permitted if the emissions released are offset by the reduction in emissions at another plant in the area [Clarke 1997].

[2] Environmental Protection Agency, United States. www.epa.gov

## 4.3 Review of Common Gaseous Environmental Pollutants

There are a large number of gaseous compounds of environmental concern, however, the list is too extensive to warrant a discussion of them all. Only major gases of environmental concern are discussed below.

### 4.3.1 Carbon Containing Gases

The two major carbon containing compounds released into the atmosphere are carbon monoxide and carbon dioxide. Other carbon containing gases, for example volatile organic compounds, are discussed in the section 4.3.2. The majority of anthropogenic inorganic carbon gases are released from the combustion of fossil fuels such as coal and petrol. Carbon dioxide is the major gas component, although carbon monoxide is released in smaller concentrations resulting from incomplete combustion.

Carbon monoxide poses a greater direct health risk than carbon dioxide, however, it is readily oxidised to carbon dioxide in the atmosphere. Carbon dioxide is a major green house gas and an increase in emissions into the atmosphere are believed to be the major player causing today's climate change. Pre-industrial concentrations of carbon dioxide were between 275 *ppm* and 285 *ppm* and have risen to 382 *ppm* in 2008[3]. An increase in concentration is believed to be due to an increase in anthropogenic carbon emissions into the atmosphere from burning of fossil fuels.

Carbon dioxide acts as a greenhouse gas by trapping infrared radiation emitted from the earths surface. This is achieved by vibrational-rotational absorption of infrared radiation by carbon dioxide (and other greenhouse gases) in the atmosphere, which is then either re-emitted isotropically or converted to translational motion which is equivalent to an increase in gas temperature.

Inhalation of carbon monoxide reduces the binding capacity of oxygen to haemoglobin in the blood, resulting in headaches, nausea, dizziness, breathlessness

[3] National Oceanic and Atmospheric Administration, United States. www.noaa.gov

and fatigue. The effects of carbon monoxide poisoning depend on the concentration and the exposure time. At high concentrations common effects can include coma or death [Bernstein 2008].

### 4.3.2 Volatile Organic Compounds (VOC)

The major anthropogenic source of volatile organic compounds in the environment is the petrochemical industry [Clarke 1997]. Volatile organic compounds are a common component found in the emissions from vehicle exhausts. They include a range of organic compounds that are typically of lower molecular weight, and are released unburned from a combustion engine due to inefficient combustion. Important volatile organic compound's include ethene, ethyne, higher aliphatic hydrocarbons, benzene, toluene and xylenes [vanLoon 2000].

Exposure to can lead to irritation of the mucous membrane, fatigue and difficulty concentrating [Bernstein 2008], while some volatile organic compound's, for example benzene, are known carcinogens [vanLoon 2000]. They also can have a negative affect on flora and fauna.

Volatile organic compound's form a major component in photochemical smog and undergo various oxidation reactions involving the hydroxyl radical, released by the photodissociation of nitrogen dioxide and ozone. These reactions lead to the formation of other harmful organic pollutants such as peroxides, aldehydes and phenols.

Methane is also considered a volatile organic compound, however, it occurs naturally at higher concentrations than the organic compounds mentioned above. Anthropogenic methane is typically a result of the extraction and production of natural gas [vanLoon 2000], however, other sources include biogenic anaerobic reactions in landfills and in agriculture. Methane is an extremely powerful greenhouse gas but its concentration in the atmosphere is still very low due to various oxidation reactions in the troposphere involving the hydroxyl radical.

### 4.3.3 Nitrogen Containing Gases

Important nitrogen containing gases include nitrogen oxides (nitrogen oxide and nitrogen dioxide), and nitrous oxide.

Nitrogen oxides ($NO + NO_2$ or $NO_x$) are commonly emitted into the atmosphere from high temperature combustion engines in vehicles and serve as the starting products to photochemical smog. When nitrogen oxides and volatile organic compounds are exposed to sunlight in the atmosphere, as mentioned above, they undergo various chemical reactions producing secondary products involved in photochemical smog. Some of the products are harmful to human health, including ozone, poly aromatic hydrocarbons (PAH), peroxides and peroxyacetic nitric anhydrides (PAN).

Exposure to ozone can cause a decrease in pulmonary function and can induce airway inflammation in both healthy individuals and those with existing chronic airways disease [Bernstein 2008]. Many polyaromatic hydrocarbons are known carcinogens, peroxyacetic nitric anhydrides cause eye irritation [vanLoon 2000], and nitrogen dioxide can cause respiratory problems especially in children and infants with asthma [Bernstein 2008]

The major source of nitrous oxide ($N_2O$) is from denitrification and the conversion of nitrate to nitrous oxide in soils and waterways. The anthropogenic component is due to the extensive use of nitrogen containing fertilisers and from animal manure which increases the nitrate available for conversion to nitrous oxide. The amount of nitrous oxide produced is increased in anaerobic conditions, and when the soil temperature and moisture levels are high. Other sources of nitrous oxide include emissions from industrial processes producing nitric acid, landfill sites, and the disposal of sewage into large water bodies [vanLoon 2000].

Nitrous oxide is a known greenhouse gas, however, concentrations are low compared to other major greenhouse gases, such as carbon dioxide. The concentration of nitrous oxide has risen to 321 ppb in 2008 from a pre industrial concentration of 270 ppb[4].

### 4.3.4 Sulphur Containing Gases

The most common sulphur containing gas of environmental concern is sulphur dioxide. Sulphur dioxide is released from various activities, including the combustion of coal containing sulphur deposits, smelting of copper, lead and zinc sulphide ores, and from the atmospheric oxidation of other sulphur containing compounds such as dihydrogen sulphide and dimethyl sulphide [O'Neill 1998]. Dihydrogen sulphide is released from salt-marsh environments from the bacterial decomposition of organic sulphur compounds. Dimethyl sulphide is biogenically produced and released from the oceans [O'Neill 1998].

Sulphur dioxide is associated with respiratory problems such as asthma and bronchitis and at high levels sulphur dioxide can even cause death [Bernstein 2008].

In the atmosphere sulphur dioxide is absorbed into water droplets and oxidised to sulphuric acid, resulting in acid rain. The effect of the acid rain depends on the surrounding ecosystems ability to neutralise the acid rain. For example, rocks containing large amounts of calcium and magnesium have a greater ability to neutralise the acid, and consequently they are more susceptible to weathering [O'Neill 1998]. In soils and colloidal material the bound metal ions are displaced by the hydrogen ions from the acid. At high enough hydrogen ion concentrations, high concentrations of metals, such as aluminium, can be displaced from the matrix. This can have adverse effects on plant life, and if released into waterways, can cause problems for aquatic flora and fauna. Acid rain, however, can also be beneficial if the soils are nutrient deficient, as sulphur is an essential nutrient [O'Neill 1998].

[4] Carbon dioxide Information Analysis Centre (CDIAC). http://cdiac.ornl.gov

Acid rain is commonly associated with the deterioration of old historical stone buildings containing calcium carbonates in some locations in the world. Limestone or marble buildings slowly dissolve and architectural designs on the buildings are consequently lost [O'Neill 1998].

## 4.4 Environmental Gas Measurement Techniques

### 4.4.1 Fourier Transform Infrared (FTIR) Spectroscopy

A common and useful gas measuring instrument is the Fourier transform infrared spectrometer (FTIR). This infrared spectrometer is much more complicated than the infrared spectrometers discussed in chapter 2.

FTIR uses the absorption of infrared radiation to determine gas concentration, and therefore, it has the ability to measure concentrations of all gases that absorb in the infrared region. This makes FTIR a very valuable technique in environmental and atmospheric gas monitoring. FTIR is used for open path monitoring where there is an open atmospheric path between the infrared source and the detector, such as the measurement of gases in industrial stack emissions. It is also used in extractive measurements where the gas is drawn through the absorption cell in the instrument [Heard 2006].

Similarly to other infrared spectrometers, FTIR measurements are influenced by the presence of water due to absorption over a large section of the infrared spectrum. Advantages of FTIR over other infrared spectrometers include an increased signal-to-noise ratio and faster response time [Heard 2006] [Smith 1996]. It is a very versatile and sensitive technique which can achieve detection limits in the parts per billion (ppb) range [Heard 2006]. FTIR instruments for atmospheric monitoring cost upwards of approximately US$80,000[5] for the basic instrument, but dramatically increases with custom variations.

[5] D & P Instruments, United States. www.dpinstruments.com

### 4.4.2 Ultra-violet Techniques

There are typically two types of ultraviolet technique: absorptive and emissive. Absorptive techniques use the absorption of ultra-violet radiation, similar to infrared absorption, to measure the concentration of a gaseous species. Emissive techniques use the emission of radiation from an excited state of a gaseous molecule to measure the concentration of that gas. The two main types of emissive techniques employed for monitoring of gaseous pollutants are fluorescence and chemiluminescence.

#### Absorption

Ultraviolet absorption spectroscopy is similar to that of infrared absorption spectroscopy. Gases that absorb in the ultraviolet region are dominantly organic molecules due to their $n \rightarrow \pi^*$ and $\pi \rightarrow \pi^*$ transitions [Cazes 2005].

The main type of ultraviolet absorption is differential optical absorption spectroscopy (DOAS) which is commonly used on balloon and aircraft platforms for atmospheric gas measurements. [Heard 2006]. Analogous to FTIR, DOAS can employ open path monitoring, or the sample can be drawn through a multi-pass cell. DOAS has a high sensitivity and can measure some atmospheric gases down to parts per trillion (ppt) level [Heard 2006].

In environmental applications ultraviolet absorption spectroscopy is dominantly used in the analysis of solutions rather than gases.

#### Fluorescence

Fluorescence is the spontaneous emission of light, resulting from the relaxation of a molecule from an excited electronic-vibration-rotation state [Heard 2006]. In a fluorescence gas analyser, ultra-violet light is directed through the sample and then blocked. The sample is excited and then light from the fluorescence process is

collected at ninety degrees to the excited beam by a photometer [Down 2005] [Clarke 1997].

Sulphur dioxide ($SO_2$) concentrations in air and stack emissions are commonly measured using ultraviolet fluorescent techniques. Other common gases that are measured using fluorescence include nitrogen oxides (NOx), polyaromatic hydrocarbons (PAH), and halogens. Fluorescence techniques can measure some gases down to parts per trillion level [Heard 2006].

### Chemiluminescence

Chemiluminescent gas analysers rely on a chemical reaction to produce the electronically excited state [Down 2005]. These analysers are dependent on a specific chemical reaction, therefore, they are typically designed specifically to measure only one gas.

In the first step, the sample is mixed with a known amount of reactant to generate the excited species. In the second step, light produced by the decay of the excited state is detected.

Chemiluminescence is commonly used to measure the concentration of total nitrogen oxides ($NO_x$) in ambient air monitoring. This is achieved through the reaction of nitrogen oxide (NO) with ozone ($O_3$). The nitrogen dioxide ($NO_2$) in the sample is converted to nitrogen oxide, by use of a molybdenum catalyst heated to approximately 300 °C, whose concentration is then determined using chemiluminescence.

Chemiluminescence has also been used to measure ozone via reaction with ethylene, and sulphur and phosphorous compounds via reactions with hydrogen. Chemiluminescent techniques can measure gas concentrations down to the low parts per million level [Clarke 1997] and currently cost upwards of approximately US$11,000[6] with a significant increase in cost with custom parts.

[6] Thomson Environmental Systems, Australia. www.thomsongroup.com.au

### 4.4.3 Solid State Sensors

There are two main types of solid state gas sensors: electrochemical sensors and conductometric sensors. Electrochemical sensors are based on solid electrolytes and conductometric sensors are based on resistant changes in semiconducting metal oxides.

#### Conductometric Sensors

A conductometric sensor is typically a semiconducting metal oxide. The most common commercialised metal oxide gas sensor is tin oxide ($SnO_2$) and was developed in the 1960's [Garcia 2004].

Conductometric gas sensors work from chemisorption of the gas onto the metal oxide surface changing the conductance of the metal oxide. Commercial conductometric devices have shown high sensitivity and can measure select gases down to parts per billion (ppb) level [Moseley 1987].

#### Electrochemical Sensors

Electrochemical sensors are similar to conductometric sensors in that they rely on the adsorption of the gas onto the surface, in this case onto the electrodes. The gas reacts with each of the electrodes in equivalent redox (oxidation and reduction) reactions producing a potential between the two electrodes through the solid electrolyte. Commercial electrochemical sensors can measure specific gases down to parts per million (ppm) level.

Electrochemical sensors have been designed to measure a wide range of gases including carbon monoxide, sulphur dioxide, hydrogen sulphide, nitrogen monoxide, nitrogen dioxide, chlorine and hydrogen chloride. The selectivity towards these gases is determined by the composition of the electrodes [Clarke 1997]. Electrochemical

sensors cost upwards of approximately US$1,000[7] depending on the gas to be measured.

### 4.4.4 Selected Ion Flow Tube (SIFT)

Selected ion flow tube mass spectrometry (SIFT-MS) is an analytical technique used for measurement of gases in air and breath samples. It uses the ionization of trace gases, by ionic precursors, to produce product ions which are measured by the mass spectrometer.

In air samples the typical ionic precursors used are $H_3O^+$, $NO^+$ or $O_2^+$ because they do not react with the major species in air ($N_2$, $O_2$, $CO_2$, and Ar), but readily react with other species in air such as volatile organic compounds and nitrogen oxides [Smith 2005] [Smith 2004]. Detection limits for the SIFT-MS instrument can be as low as the parts per billion level.

The major advantage of SIFT-MS is its ability to analyse complex gas mixtures in air samples simultaneously and in real time. A sample spectrum for an air sample can be achieved in only thirty seconds [Smith 2004]. Another advantage, compared to gas chromatography mass spectrometry (GC-MS), is that SIFT-MS does not require collection of gas sample onto absorption traps or bags which can result in the degradation of the sample.

SIFT-MS instruments cost upward of US$200,000[8], are expensive on consumables, require a dedicated trained operator and are of limited portability. Completely portable SIFT-MS instruments are yet to be produced with partially portable instruments available which require a mains power supply [Smith 2005].

[7] Detcon Inc. www.detcon.com
[8] Syft Technologies Ltd. www.syft.co.nz

### 4.4.5 Gas Sampling and Separation Techniques

#### Sampling Probes

Some measurements of trace gases must be carried out by extracting a sample and transporting it to a gas analyser. This is especially so with industrial emissions from flues or chimneys. It is essential that the sample of gas presented to an analyser is representative of the gas present in the process stream at the sampling point. This has obvious legal significance in the case of measurements undertaken to demonstrate compliance with an emission limit [Clarke 1997].

The sampling probes are generally made out of stainless steel because it can withstand temperatures up to 600 °C and is resistant, to some extent, to erosion caused from particulates. At higher temperatures special alloys or ceramics are used. The inner tube of the probe is made of a material which is resistant to the gases in the sample. For example, $H_2SO_4$ vapour is best sampled with a silica-lined tube because heated metal acts as a catalyst for the reaction of $SO_2$ to $SO_3$. Similarly, HCl vapour should be sampled with PTFE or glass as it also undergoes reactions with stainless steel [Clarke 1997].

Water cooled probes are occasionally used for high temperature sampling as the cooling quenches any further reactions taking place during transportation of the sample [Clarke 1997]. The transfer lines from the probe are normally heated to avoid condensation. The temperature at which the transfer line is heated depends on the composition of the gas sample. The transfer lines are generally made of a Teflon core surrounded by a heating coil and insulation [Clarke 1997].

#### Gas Chromatography

Gas chromatography is a method of continuous separation of one or more individual compounds between two phases [Down 2005] and has been coupled with a range of gas sensors. In general, the two phases consist of a stationary phase and a mobile phase. The stationary phase is a solid contained in a column through which the mobile

phase flows. The gases are separated depending on their vapour pressure. Compounds with high vapour pressure are eluted first and compounds with low vapour pressures are eluted last. The lower the vapour pressure the longer the compound will remain in the stationary phase.

A range of detectors have been used to detect the gases as they elute from the GC column. These detectors include: flame ionisation detector (FID), photo-ionisation detector (PID) and Electron capture detector (ECD).

The flame ionisation detector is used mostly for the determination of hydrocarbons including some volatile organic compounds. FID coupled with GC can have detection limits as low as 1 ppb with a linear response of up to seven orders of magnitude. The photo-ionisation detector is approximately ten to one hundred times more sensitive than the flame ionisation detector [Down 2005]. It also has the ability to measure inorganic compounds which flame ionisation cannot. The electron capture detector is used specifically to measure chlorinated hydrocarbons and has detection limits down to 0.1 ppb.

## 4.5 Discussion

There are many factors influencing which instrument is the "best". The type of analytical instrument chosen depends largely on the budget set towards gas monitoring, what the instrument will be used for, and any legal requirements there may be.

Typically, the less expensive the gas analyser the lower its ability to measure more than one gas. Cheaper gas analysers tend to be small, portable devices whose sensitivity may match that of more expensive instruments, but measurements are restricted to a single gas. An increase in versatility results in a dramatic increase in the price. For example, solid state electrochemical sensors and chemiluminescent analysers are portable and reasonably affordable but are specifically designed for

single gas measurements, whereas, FTIR instruments are expensive (by 100-fold), not portable, but very versatile.

The most expensive instrument is the selected ion flow tube mass spectrometer which would be regarded as the best analytical instrument for gas measurement. It has a very fast response time, high sensitivity, and does not have interferences by major components in the air samples. However, SIFT-MS has a high cost which is likely to be out of the budget range for most small companies, and has limited portability reducing its use in remote locations without a mains power supply.

It can be seen that there are no portable, moderately inexpensive instruments on the market which demonstrate a high sensitivity and multiple gas measurement. There is a large gap in the cost between the less expensive single-gas analysers and the expensive multi-gas analysers.

## 4.6 Summary

Much work in the advancement of analytical technology is needed to produce an inexpensive gas analyser which can be used to achieve compliance for emissions monitoring of numerous gases. Due to the legal requirement of emissions monitoring in most countries, there is a high demand for this type of inexpensive gas analyser.

# Chapter V

# Instrument and Modifications

## 5.1 Introduction

This research project is based on the development of a non-dispersive infrared instrument designed and implemented in a previous research project. This chapter discusses the design and specifications of the original instrument, and modifications made to the instrument in order to restore it back to working order. Once restored to working order, preliminary measurements of three atmospheric gases, carbon dioxide, methane and nitrous oxide, were measured before further instrumental developments took place.

## 5.2 The Original Instrument

The original instrument was designed by Mark Bart, and constructed by Timothy Simpson in 2004. The design was based on the positive filter non-dispersive infrared analyser discussed in Chapter 3. Two chambers are incorporated into the instrument housing, a source chamber and a detection chamber. Infrared sources are enclosed in the source chamber, and gas cells and a luft type detector are enclosed in the detection chamber. These are discussed in detail later in this chapter. Figure 5.1 illustrates a schematic diagram of the original non-dispersive infrared analyser.

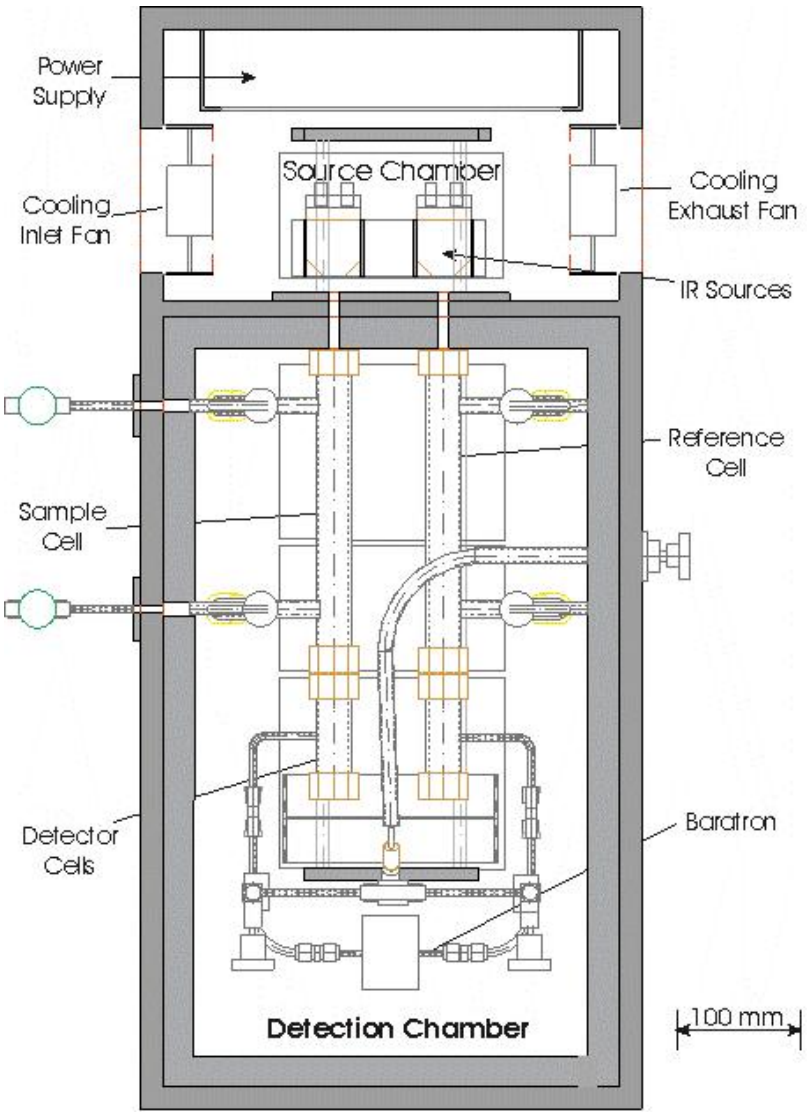


**Figure 5.1**: Schematic of original non-dispersive infrared analyser [Simpson 2004].

### 5.2.1 Instrument Housing and Electronics

The instrument housing is made out of medium density fibreboard (MDF) and measures 885 *mm* in length, 403 *mm* wide and 213 *mm* in height. The lid, which is also made from medium density fibreboard, carries a small boxed addition for a temperature controller. 25 *mm* polystyrene lines the walls of the housing. On the inner base of the instrument housing there are four Teflon tables mounted on two parallel aluminium alignment rods. One table is in the source chamber for the alignment of the infrared sources, and three are in the detection chamber for the alignment of the sample and reference gas cells and the detector cells. Two 8 *mm* diameter circular

apertures made from stainless steel tubing pass through the interface between the chambers for the transmission of infrared radiation from the infrared sources into the detection chamber.

The temperature controller is mounted on the lid of the instrument and consists of a fan, a heating wire and electronics. A temperature sensor is mounted within the detection chamber and continually measures the temperature which is displayed on an LCD screen on the instrument lid. The temperature can be manually adjusted by a dial inside the lid and can operate between 26 °*C* and 42 °*C*. All electrical components are operated from a single 240 *V* power supply.

### 5.2.2 Infrared Sources

The two original infrared sources are made from 19 gauge nichrome wire in the form of coils, formed by winding the wire eight times around a 7 *mm* diameter core. 22 gauge copper was wound around the filament support legs and attached with silver solder. A ceramic and metal casing, with a persplex base, houses the filaments. The two sources are connected in parallel with eight 100 *Ω* resistors connected in series. Figure 5.2 illustrates a diagram of the nichrome wire filaments and the infrared source casing.

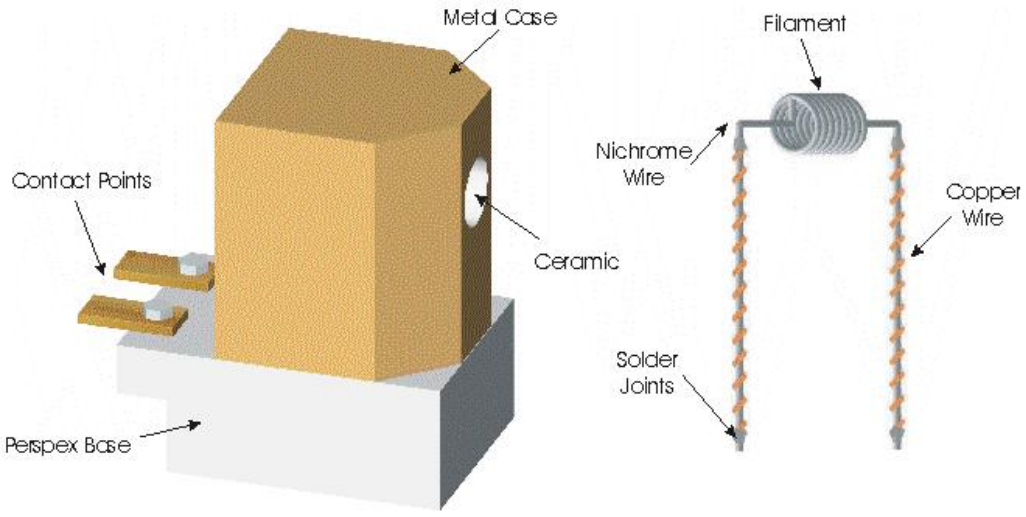


**Figure 5.2**: Infrared source casing and nichrome wire filament [Simpson 2004].

Two fans located in the source chamber, one directing cool air into the chamber and one extracting warm air out, minimize the temperature difference between the chambers. The fans and the infrared sources all operate on a 5 $V$ power supply also located in the source chamber.

Fairyboard, a heat absorbing fibre board, is located between the infrared sources and the detection chamber to minimises the heat transfer into the detection chamber from the infrared sources.

### 5.2.3 Gas Cells

There are two gas cells in the instrument, a sample cell and a reference cell. These gas cells are made of glass and are sealed at each end with infrared transmitting KRS-5 (Thallium iodide – Thallium bromide mix) windows. The windows are held in place with brass screw-fit locking caps and sealed with rubber o-rings. Figure 5.3 illustrates the fitting of the windows in the gas cells.

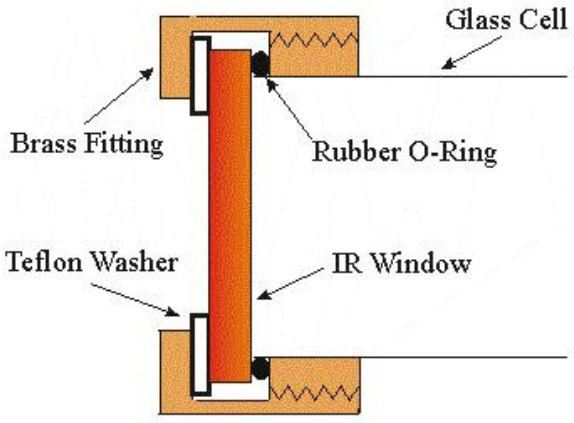


**Figure 5.3**: Diagram of window fitting, in the gas cell [Simpson 2004].

The sample and reference cells each have two ¼" glass to metal seals for gas transfer in and out of the cell, these are connected to the gas handling line through Young's valves.

### 5.2.4 Infrared Detector

The infrared detector is a luft-type device in which small differences in pressure on either side of the diaphragm of an MKS model 233, 0.02 *Torr* full-scale, Baratron differential capacitance manometer are measured The capacitance manometer is connected to two gas cells which are made from glass and fitted with KRS-5 windows sealed with brass fittings similar to the gas cells mentioned above, as shown in figure 5.4. The gas cells are connected to the baratron by ¼" stainless steel tubing and the two cells are separated by a Whitey needle valve. This valve is operated from outside the instrument housing through a Bowden cable. A swagelock valve is connected to each side of the Baratron to allow the filling of the detector cells.

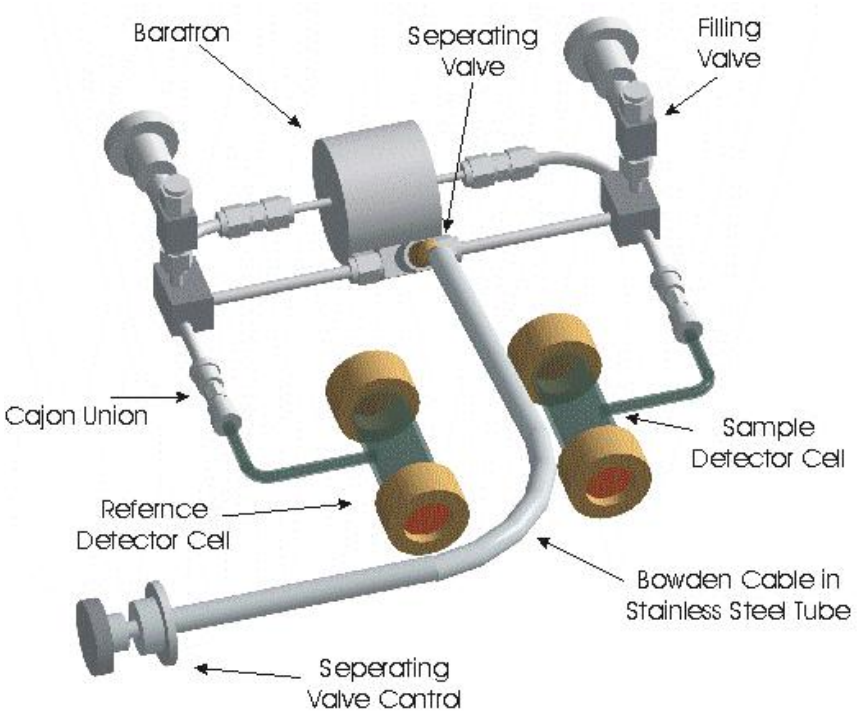


**Figure 5.4**: Luft-type detector apparatus [Simpson 2004].

### 5.2.5 Gas Delivery Line

The gas delivery line, shown in figure 5.5, is made of ¼" stainless steel tube with swagelock fittings and is mounted on a 455 *mm* x 660 *mm* trolley with a 1800 *mm* high supporting frame. A mechanical pump and turbo-molecular pump are mounted in the base of this frame, providing vacuum for the entire line. Two small gas tanks are installed and connected to the gas line for gas sample and gas mixure preparation, and a 1000 *mbar* Baratron differential capacitance manometer is connected to measure the pressure in the line.

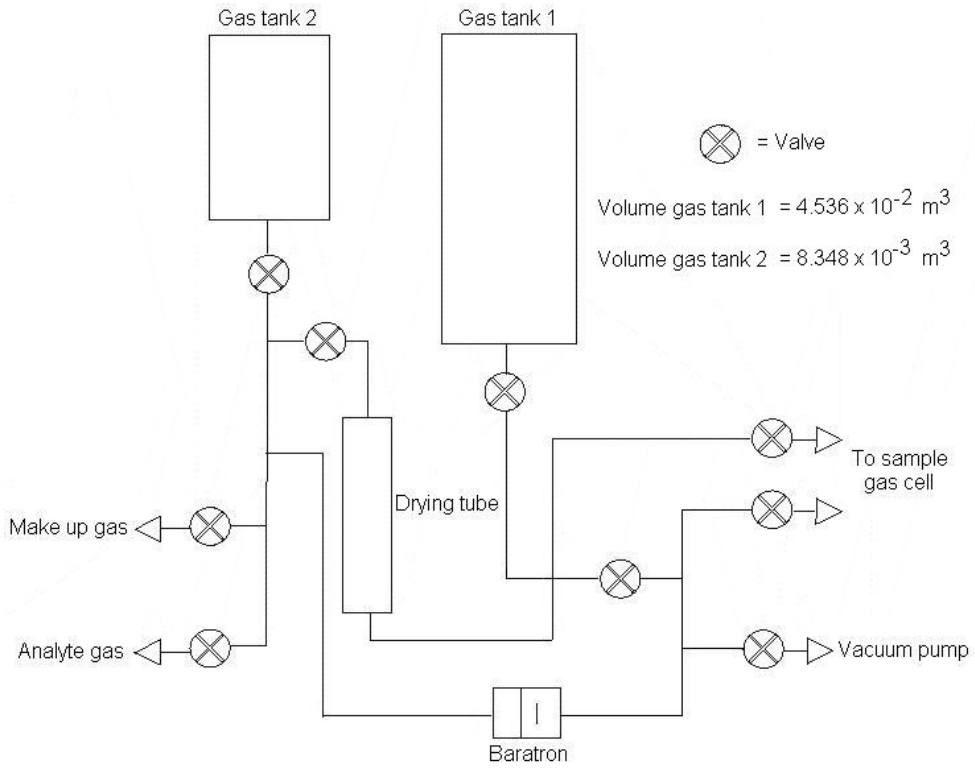


**Figure 5.5**: Schematic of original gas delivery line.

## 5.3 Instrument Modifications

Many changes to the original instrument were made in an attempt to refurbish the instrument back to working order, and to overcome problems identified in the prototype instrument. Other small changes were also completed to increase the ease of operation of the instrument and to further reduce the overall fabrication cost.

### 5.3.1 Infrared Sources

The power supply to the infrared sources was modified by removal of the panel of ballast resistors and the addition of a manual voltage controller. This allows manual regulation of the current across the infrared sources, altering the operating temperature of the infrared sources. The voltage to the filaments can be varied from 3.9 $V$ to 5.4 $V$, corresponding to a range from very low IR emission through to filament meltdown, respectively.

A small slit was made in the lid of the instrument to allow a metal slide to be inserted in front of the infrared sources in order to block the radiation from entering the detection chamber. This significantly reduces the energy absorbed in the detector between measurements, and removes the requirement to continually turn the infrared sources on and off. The metal slide can be inserted and removed without removing the lid of the instrument and influencing the temperature equilibrium in the detection chamber.

The original infrared filaments were highly oxidised, resulting in a low energy output that was inadequate to produce a response from the detector containing carbon dioxide gas. New infrared filaments, illustrated in figure 5.6, were hand made to a similar design as the original infrared filaments. They were made from identical lengths of 19 gauge nichrome wire with a central coil wound eight times around a 5 *mm* diameter core. Copper wire was wrapped around the filament support legs and soldered on.

**Figure 5.6**: Hand made nichrome wire infrared filaments.

The infrared sources exhibit a resistance of approximately 0.3 $\Omega$ and operate at a maximum temperature difference of around 50 $°C$. Figure 5.7 illustrates the temperature profile for the infrared sources with increasing filament voltage supply. The temperature of the filaments was measured using an optical pyrometer.

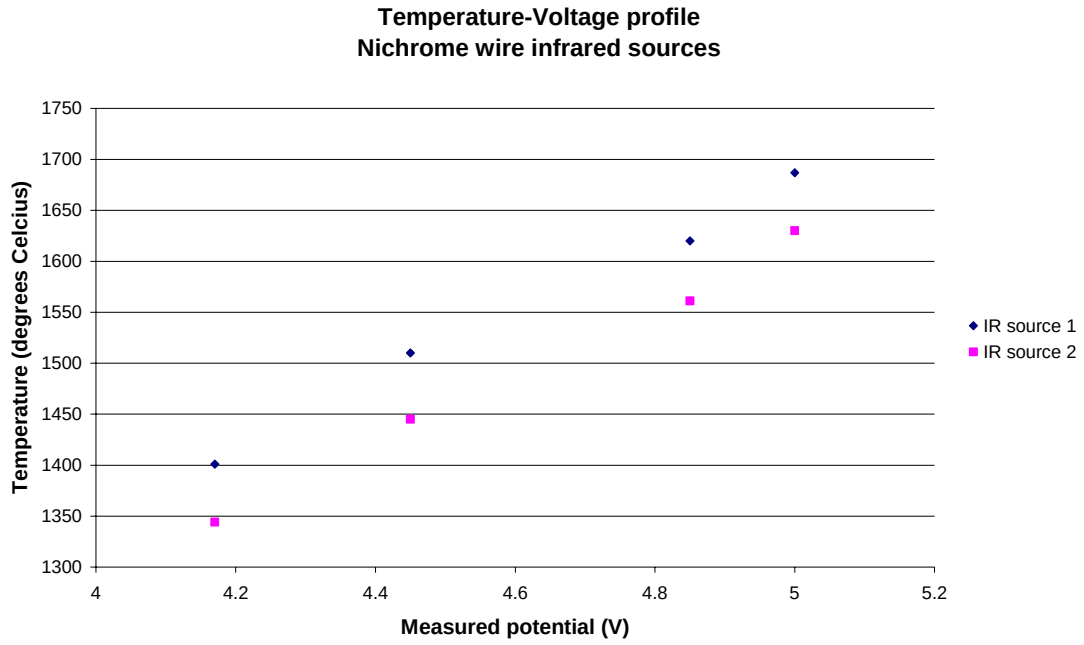


**Figure 5.7**: Temperature – Voltage profile for each infrared source.

The differences in temperatures for the two sources will lead to one side of the detector heating faster than the other, giving rise to an increasing or decreasing baseline. Although the changing baseline can be removed mathematically using

Excel, the insertion of a card restricting the beam profile in front of the infrared source with the higher temperature kept the changing baseline to be minimum. In addition, the sources could be interchanged within the source chamber and this also affected the baselines as shown in figure 5.8 which illustrate the differences in baselines for changing infrared source positions.

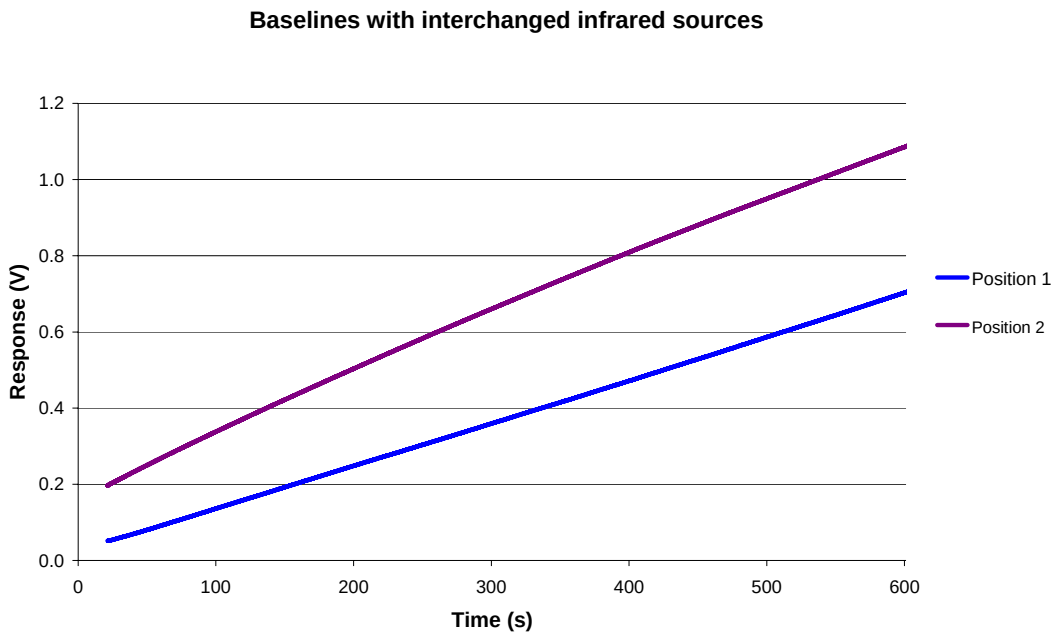


**Figure 5.8**: Baseline measured with infrared sources interchanged.

Position 1 refers to the infrared sources in an arbitrary position when the source labelled 1 is on the reference side and the source labelled 2 is on the sample side. Position 2 is when the sources are interchanged.

### 5.3.2 Gas Cells

The optical windows in the gas cells were replaced due to a high degree of degradation and formation of f-centers. Infrared windows used to replace the original KRS-5 windows were salvaged from the Department Instrument Laboratory and were believed to be either sodium chloride or potassium chloride. The window material was determined using a Perkin Elmer FT-IR analytical spectrometer, to measure the transmission spectrum of the window, and qualitative inorganic analysis to confirm

the result. An infrared spectrum of each of the windows was obtained and compared to the spectra of known infrared transmitting materials. Figure 5.9 shows the measured infrared spectrum of one of the windows.

A small shaving of the window was dissolved in water, with the addition of silver nitrate ($AgNO_3$). The formation of a white precipitate of silver chloride (AgCl) concluded the presence of the chlorine anion. A second test was then conducted to determine the respective cation using sodium hydrogen tartrate solution. A small shaving of the window was dissolved in sodium hydrogen tartrate solution with fifty percent ethanol. In the presence of potassium the following reaction occurs [Vogel 1996].

$$K^+ + H_2C_4H_4O_6 \rightarrow KHC_4H_4O_6 + H^+ \qquad 5.1$$

The formation of the white crystalline precipitate of $KHC_4H_4O_6$ indicated the presence of the potassium cation. The chemical and spectroscopic analyses of the windows confirmed the window material as potassium chloride.

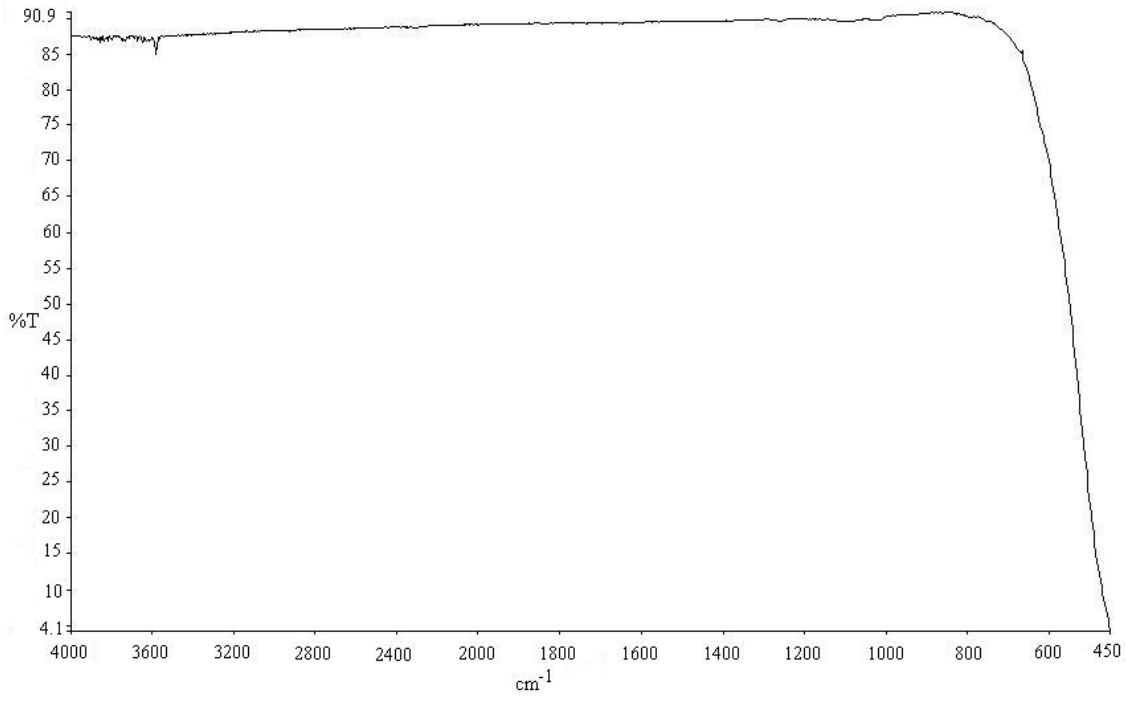


**Figure 5.9**: Percent transmittance versus wave number for a KCl infrared window.

Potassium chloride windows are a better choice as infrared transmitting windows than KRS-5; they are less expensive (US$80.00 for potassium chloride windows compared with US $170.00 for KRS-5 windows[9]) and have a greater transmittance over a wider wavelength range in the infrared region. Potassium chloride windows, however, are hygroscopic and are prone to fogging in high humidities. This problem was significantly reduced by placing small aerated bags containing silica gel desiccant in the detection chamber, which can be easily fitted around the gas cells or in tight corners. Silica gel was chosen over calcium chloride because it can be reused and because it includes moisture saturation indicative properties. At high saturation, calcium chloride dissolves requiring a solid support to collect the liquid slurry, whereas silica gel does not dissolve and can be used in the aerated bags making it a more practical choice.

### 5.3.3 Infrared Detector

The MKS Baratron differential capacitance manometer in the detector unit was initially found to be faulty and would not respond to changes in pressure on either side of the diaphragm. It was sent to the United States to be refurbished and during this time an older MKS Baratron differential capacitance manometer was used in the detector unit. Unfortunately, due to differences in sizes between the two Baratrons, problems arose with reseating the detector cells. The detector cells were not in-line with the infrared sources and had to be re-shaped by the glass blower. This procedure then had to be reversed when the original unit returned from MKS.

### 5.3.4 Inconsistent Baselines

A problem arose after the refurbished Baratron was reinstalled into the instrument; the baseline was varying from day to day. The inconsistencies included parabolic baselines, linear baselines, and both negative and positive baselines being recorded. It was found that the power supply to the Baratron had been sitting next to the exhaust fan from the source chamber which was causing a large variation in temperature over

[9] ISP Optics E-Store. www.ispoptics.com

during the day which was initially suspected to be causing differences in the Baratron signal resulting in the inconsistent baselines. However, when the power supply was moved away from the exhaust fan the inconsistencies continued.

The problem was caused from a heating effect, which was diagnosed when the inconsistencies in the baseline disappeared after the internal detector housing temperature regulator was kept in operation continuously for a period of two weeks. It was concluded that the baseline variations were due to differences in the mass of glass in each of the detector cells. The differences in mass resulted from the adjustments made when reseating the glass cells following the swapping of Baratrons in the detector unit. Due to the low thermal conductivity of glass, it took a long time for both glass cells to reach thermal equilibrium. Dramatic changes in temperature in the laboratory affected the temperature in the detection chamber. Many variations in the baseline arose from the slow response of the glass cells to these temperature changes.

### 5.3.5 Gas Delivery Line

The gas delivery line was modified to increase the ease of gas sample preparation and delivery into the sample cell. Additions to the gas line were plumbed in copper tubing since there were no plans to use corrosive gases that might attack copper.

A connection was made between the two gas cylinders to bypass the drying tube. The drying tube is only required to remove moisture from samples but is not required for the measurement of dry standards. The drying tube contains calcium chloride desiccant which absorbs moisture from the sample. An additional valve and extra blanks in the gas line were added for ease of modification in the future. Figure 5.10 illustrates a schematic diagram of the redesigned gas delivery line.

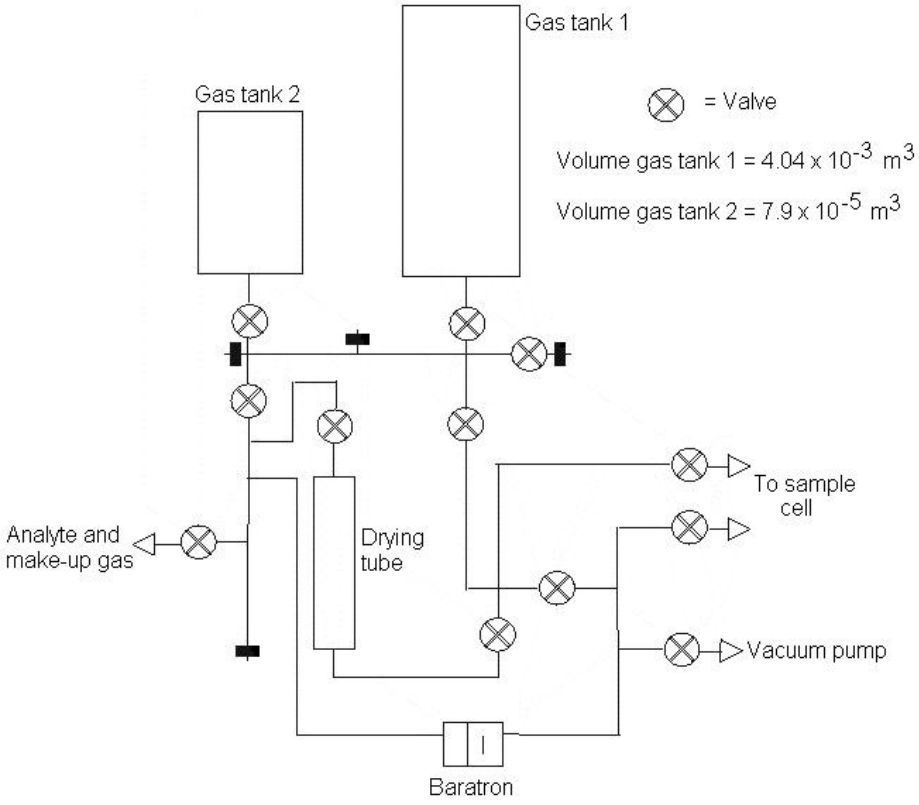


**Figure 5.10**: Schematic of redesigned gas delivery line.

The volume of the largest gas tank (gas tank 1) was determined by weighing the empty cylinder and then weighing the gas cylinder when full of degassed distilled water. The volume was calculated from the density of water corresponding to the temperature of the water. The other sections of the gas handling system were determined by expanding gas from the calibrated gas tank into the gas line using Boyle's law:

$$P_1V_1 = P_2V_2 \qquad 5.2$$

Where P = Pressure of the gas

V = Volume

# Chapter VI

# Instrumental Developments

## 6.1 Introduction

This chapter describes the instrumental developments completed in order to improve the sensitivity and performance of the instrument.

A number of changes were made, including the addition of a beam chopper to the source chamber and the incorporation of a new cooling system in the detection chamber.

## 6.2 Beam Chopper

The beam chopper, shown in figure 6.1, consists of a stepping motor and an aluminium chopper blade. The chopper blade measures 100 *mm* in length in order to alternatively pass and block the IR beams by covering the collimators, between the source chamber and detection chamber, as the blade rotates. The chopper blade is mounted and aligned with an aluminium stand and attached to the stepping motor with rubber tubing. The stepping motor was salvaged from the electronics workshop, possibly from an old computer hard drive.

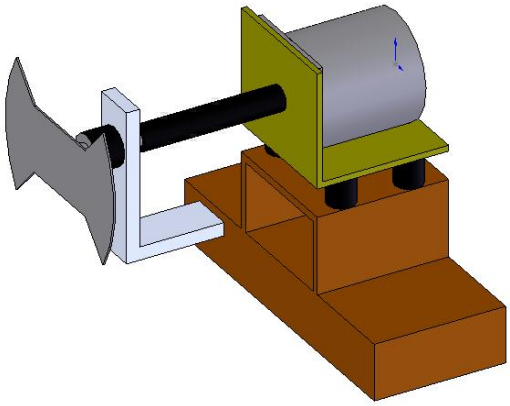

**Figure 6.1**: Schematic of beam chopper.

The upper frequency for the beam chopper is 2.5 *Hz*, attempts to increase above this frequency result in a decrease in frequency as the stepping motor begins to miss steps. It is used in conjunction with an analogue lock-in amplifier to improve the signal-to-noise ratio. An infrared switch, used as a counter, located directly above the chopping blade on the wall separating the source and detection chambers, measures the chopper frequency. The blade of the chopper passes through the counter blocking a small infrared beam and breaking the photoelectric circuit. This produces TTL (5 V) pulses when the IR beam unblocked (chopper open) and 0 V when the beam is blocked (chopper closed). The square wave signal from the switch, corresponding to the frequency of the beam chopper, is used to trigger the lock-in amplifier.

Due to the large size of the chopper, a number of changes to the source chamber where required. To increase space in the source chamber the power supply, for the infrared sources and fans, was relocated to the outside wall of the source chamber. This change not only allowed room for the stepping motor, but also allowed better control of the infrared source temperature as the voltage controller was now located outside of the instrument. The modified source chamber is illustrated in figure 6.2.

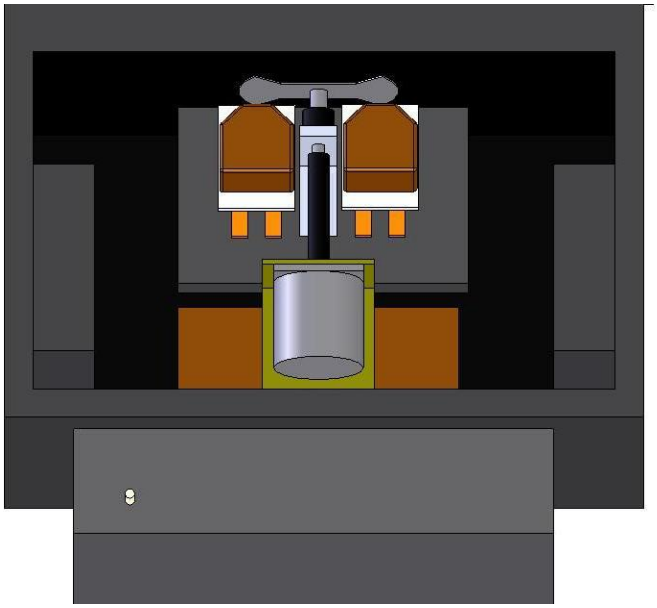

**Figure 6.2**: Schematic of modified source chamber.

When the beam chopper was placed in the source chamber, the infrared sources were moved back slightly to allow the chopper blades to rotate freely between the sources and the apertures. This, however, results in a decrease in the infrared radiation reaching the detection chamber. This loss of radiation was partially overcome by increasing the electric current to the sources and increasing the source operating temperature and the IR intensity.

## 6.3 Temperature Regulation

Unstable baselines arising from changes in temperature in the detection chamber continued to cause problems when obtaining a measurement. The inefficiency of the temperature regulator resulted in large temperature variations observed on a daily basis. A number of solutions were proposed, including changing the detector cells to a different material, for example, ceramic, and an alternative cooling system for the glass cells. A cooling sleeve was designed and made to fit around the glass detector cells. The cooling sleeve, shown in figure 6.3, is made of aluminium in two halves. Each half contains a hollow cavity which was milled out of the aluminium, with two ¼” diameter tubes for water in and water out. The two halves are clamped around the detector cells and held tightly in place with o-rings stretched over the two halves.

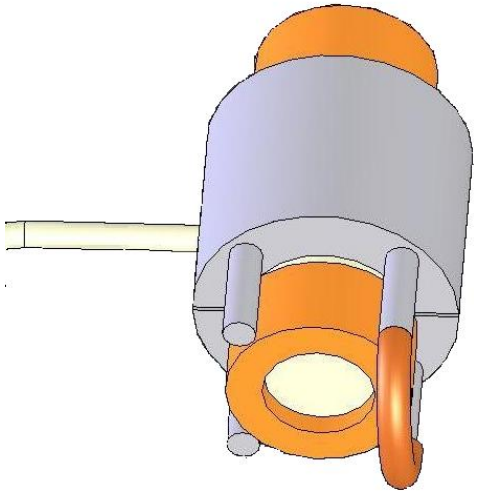

**Figure 6.3**: Detector cells cooling system.

Water from the mains water supply, which was measured to be a constant 17 °*C*, is pumped through plastic tubing to the instrument casing. At this point the tubing separates to service each cooling sleeve individually. The water passes through the bottom half of the cooling sleeve and through a copper pipe into the top half of the cooling sleeve. The water is then removed through plastic tubing, where it is combined with the used water from the other cooling sleeve, and is removed from the instrument. The water is pumped from bottom to top to avoid air bubbles in the cooling sleeve which may hinder its temperature regulating performance or cause vibrations which could affect the baseline. The gas cells which sit between the two halves of the cooling sleeve are propped up to the appropriate height with polystyrene.

## 6.4 Lock-in Amplifier

The signal from the Baratron is passed through a home-built differential dc amplifier, which gives a thirty times gain on the signal, and into the lock-in amplifier. The lock-in amplifier is a Stanford Research Systems model SR5 10. It receives the alternating voltage output from the Baratron corresponding the IR-on (chopper open) and IR-off (chopper closed). The reference signal is the voltage signal from the counter which corresponds to the chopper frequency. The sample signal is modulated, filtered and then cross-correlated with the reference frequency. The Baratron signal passes through a low band-pass filter, producing an intensified output signal from the lock-

in amplifier [Ewing 1997] after establishing the best phase shift to use (between chopper signal and detector signal).

The lock-in amplifier produces a flat baseline from the differences in the two measured signals from the Baratron. This removes the requirement to mathematically subtract the increasing (or decreasing) baseline. The baseline contains a large amount of random noise which can be removed either by mathematically averaging the data, or by reducing the sensitivity on the lock-in amplifier to give reduced noise. However, this noise does not cause problems during data collection or analysis.

## 6.5 Instrument Operation

The beam chopper is limited to operating frequencies below 2.5 *Hz*. However, the lock-in amplifier can only "lock-in" at frequencies above 1.49 *Hz*, resulting in an instrument operating frequency range for the beam chopper of 1.49 *Hz* to 2.50 *Hz*.

It was found that the sample frequency (Baratron signal) must be close to 60° out of phase of the reference (chopper) frequency on the lock-in amplifier to achieve an optimum signal response. The phase can be determined by scrolling through the phases while a sample is in the sample cell until a maximum signal is observed. The phase must be changed if the chopping frequency is altered. Figure 6.4 illustrates the change in response for a 500 *ppm* nitrous oxide standard for different phases at a chopping frequency of 1.49 Hz.

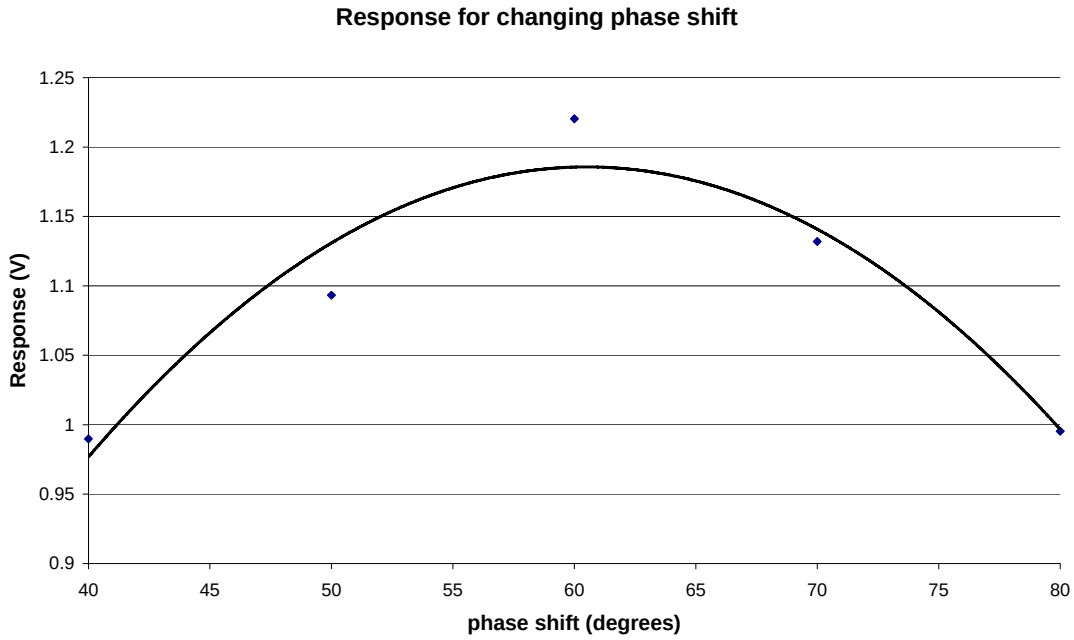


**Figure 6.4**: Response for a 500 *ppm* standard for different phases and constant chopping frequency of 1.493 *Hz*.

The response from a 500 *ppm* nitrous oxide standard was measured for a small range of chopping speeds to determine the optimum frequency for best response. At a chopping frequency of 1.49 Hz a maximum response was found with a phase shift of 62.1 degrees.

When the chopping frequency was increased the phase was changed on the lock-in amplifier to get the greatest signal response for that frequency. Table 6.1 illustrates the chopping frequencies, optimum phase, and the signal response from the 500 *ppm* nitrous oxide standard for three different chopping frequencies.

| Chopping frequency (Hz) | Response (V) | Phase (degrees) |
|---|---|---|
| 1.5 | 1.290 | 62.1 |
| 2 | 0.911 | 75.3 |
| 2.5 | 0.829 | 69.1 |

**Table 6.1**: Comparison of signal response for different chopping frequencies.

Table 6.1 indicates that signal response increases with decreasing chopping speed. The absorption of infrared radiation in the detector cells is not instantaneous and is a limiting factor (similarly for relaxation when the infrared sources are blocked). At higher chopping frequencies the difference between the two signals is reduced because the gas in the detector cells have only limited time for relaxation to occur after being excited. Also, a fast chopping frequency reduces the time for the gas in the detector cells to absorb infrared radiation, heat the gas in the cell, and increase the pressure to be measured by the Baratron. Figure 6.5 illustrates the change in optimum response at the three chopping frequencies.

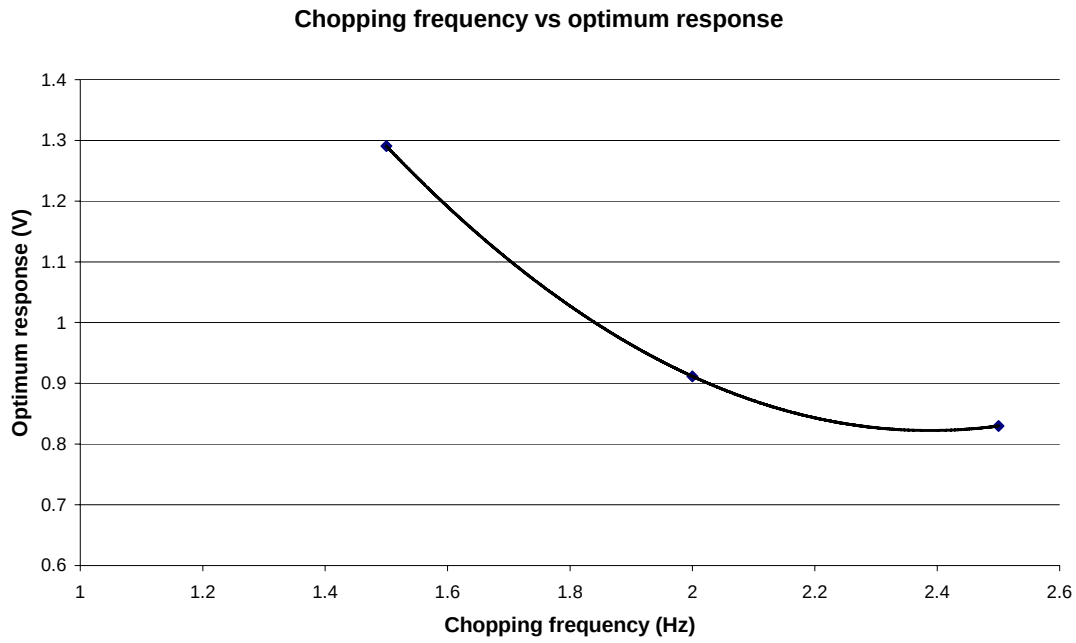


**Figure 6.5**: Response from Baratron with different chopping frequencies.

## 6.6 Instrument Cost

Table 6.2 shows an outline of the instrument cost in US dollars, where NZ$1 = US$0.60. The total price to construct this instrument is approximately US$3,350.00 which is relatively inexpensive compared to current commercial gas analysers.

| **Instrument Cost** | | | |
|---|---|---|---|
| **Casing** | | | |
| | Instrument Case | **$** | 40 |
| | Optical Table | **$** | 35 |
| **Source Chamber** | | | |
| | Power Supply | **$** | 44 |
| | Cooling Fans | **$** | 40 |
| | Infrared Sources | **$** | 47 |
| | Beam Chopper (Including stepping motor) | **$** | 150 |
| **Electronics** | | | |
| | Baratron Power Supply | **$** | 38 |
| | Voltmeter with PC Interface | **$** | 384 |
| | DC Amplifier | **$** | 70 |
| | SR5 10 Lock-in Amplifier[10] | **$** | 2500 |
| **TOTAL** | | **$** | **3348.00** |

**Table 6.2**: Cost of the components of the instrument.

Figure 6.6 and figure 6.7 show a schematic diagram and a three dimensional diagram of the final instrument, respectively.

[10] Stanford Research Systems. www.thinksrs.com

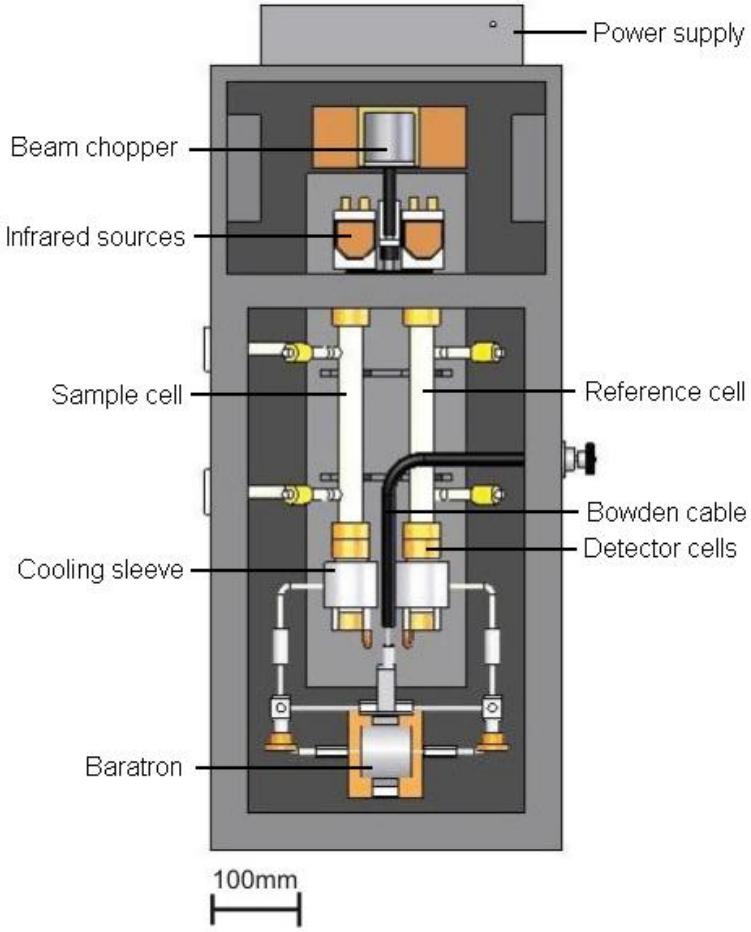


**Figure 6.6**: Schematic of final instrument.

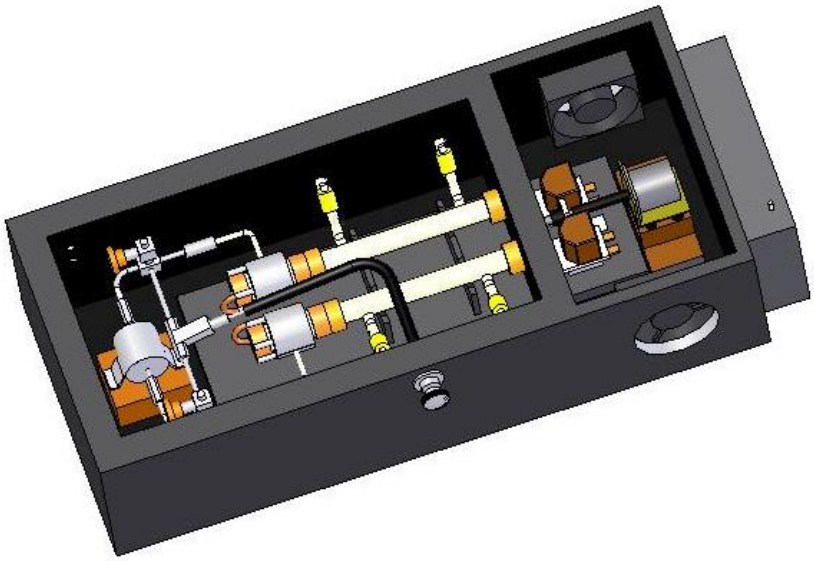

**Figure 6.7**: Three dimensional diagram of final instrument.

## Chapter VII

# Instrument Results

## 7.1 Introduction

Measurements of standards were carried out to determine the sensitivity and response of the instrument for trace gas analysis. Three gases were used as analyte gases for standard measurements; carbon dioxide, methane, and nitrous oxide. These gases were selected because they absorb strongly in the infrared region and are common greenhouse gases released due to industrial activity, transport and intensive farming. This chapter contains calibration graphs for all three gases, detection limits for the instrument for each of the gases, and the measurement of $CO_2$ in laboratory air samples.

Initial standard measurements were carried out after the instrument was refurbished back to working order. These results are not discussed here as they are only preliminary results. Further standard measurements were then completed after the final instrument modifications were finished, as discussed in chapter 6. These results are discussed below.

## 7.2 Statistical Analysis and Instrument Response

### 7.2.1 Statistics

For each gas the detection limit, limit of quantitation, and limit of linearity were determined. These are briefly discussed below, and all statistical equations are shown in Appendix B.

The detection limit (DL) is the minimum concentration of an analyte that can be detected at a known confidence level. The detection limit is calculated at this confidence level from linear regression as being the intercept of the line plus three times the standard deviation.

The limit of quantitation (LOQ) is the lowest concentration at which quantitative measurements are made. The limit of quantitation is calculated using linear regression as the intercept value plus ten times the standard deviation of the intercept.

The limit of linearity (LOL) is the upper quantitation limit for which the sample is measured. It is the point where the calibration graph becomes non-linear. The limit of linearity only signifies the upper limit to the linear operating range of the instrument. Since trace level analysis was the focus of the project this value is not particularly important, especially if the LOL is large.

### 7.2.2 Instrument Response

Figure 7.1 illustrates the response for a 1,000 *ppm* nitrous oxide standard from the instrument. The combination of beam chopper and lock-in amplifier removes the increasing baseline observed from the original instrument.

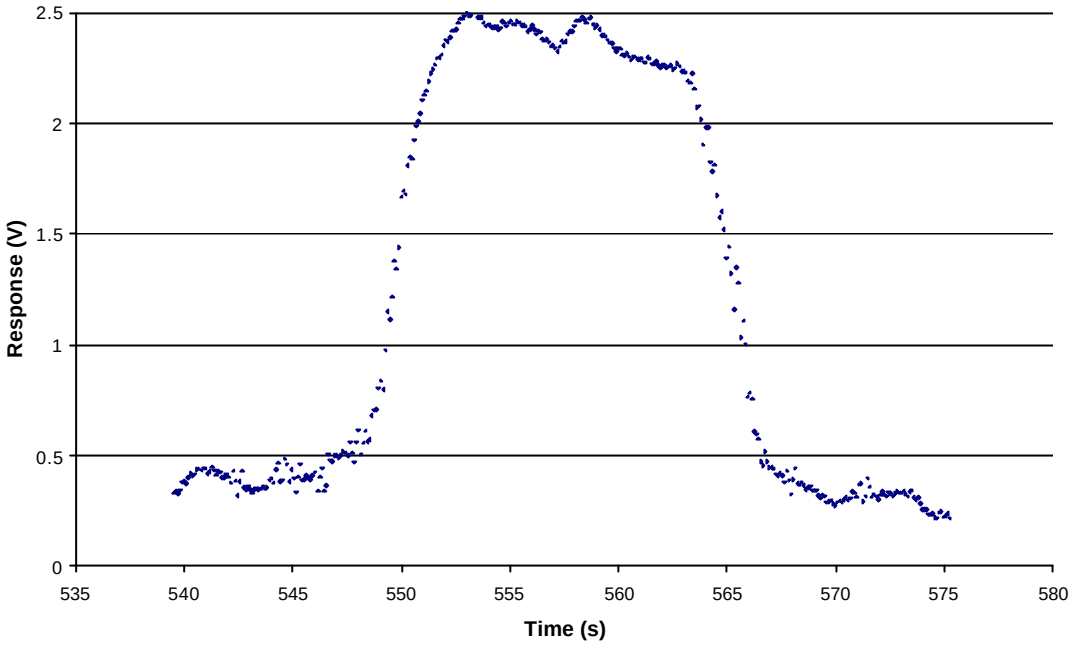


**Figure 7.1:** Response for 1,000 *ppm* nitrous oxide standard.

## 7.3 Calibration Graphs and Detections Limits

The following results were obtained from the instrument. A series of standards ranging from 40 *ppm* to 1,000 *ppm* were made up in the gas delivery line using instrument grade gases. The upper detection limit was conservatively stated at 1,000 *ppm* because measurements above this concentration would not be classified as a trace gas measurement. However, if measurements above this concentration were required a calibration graph could be easily determined in order to establish the upper limit of linearity for the instrument.

The make up gases used were argon for carbon dioxide and nitrous oxide, and nitrogen for methane, and each standard mixture allowed five measurements at one atmosphere pressure to be completed. The five measurements for each standard were averaged and a calibration graph for each gas was established.

### 7.3.1 Nitrous Oxide

Nitrous oxide measurements without the 30x signal amplifier were completed in order to determine the detection limit and the limit of quantitation. The calibration graph without the amplifier connected is shown in figure 7.2.

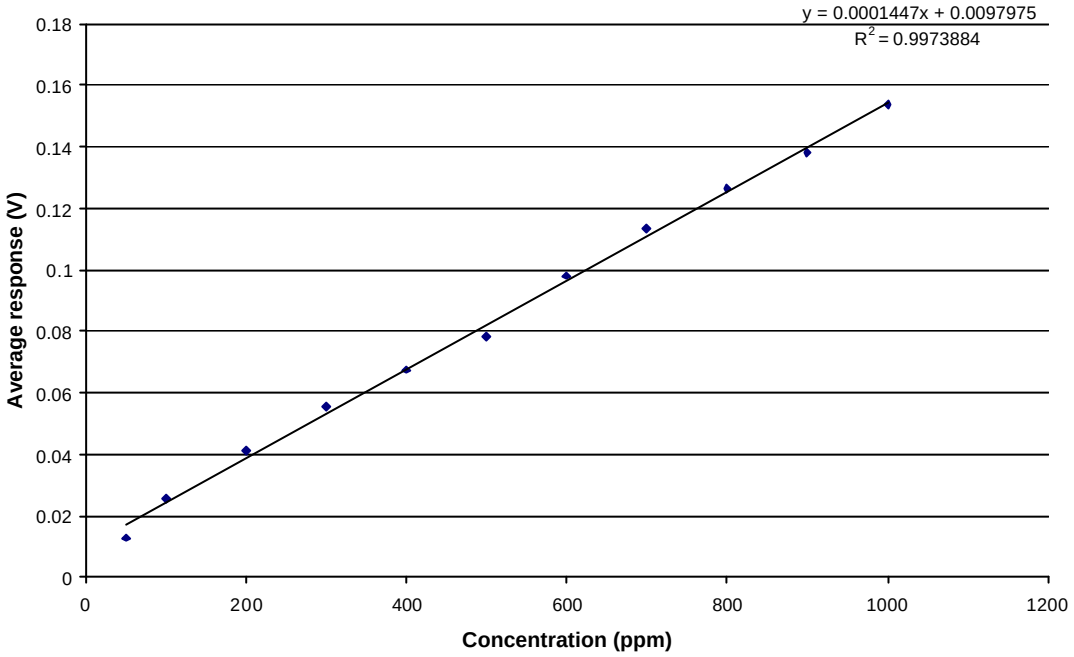


**Figure 7.2**: Calibration graph of nitrous oxide standards without 30x amplifier.

The limit of quantitation (LOQ) was calculated to be 0.01460 *V* corresponding to a concentration of 100.91 *ppm*, and the detection limit was calculated to be 0.00438 *V* corresponding to a concentration of 30.27 *ppm*. A linear relationship with an $R^2$ of 0.997 is observed over the 50 *ppm* to 1,000 *ppm* range.

Nitrous oxide standards were remeasured to determine the relative detection limits with the 30x amplifier connected. The calibration graph is shown in figure 7.3.

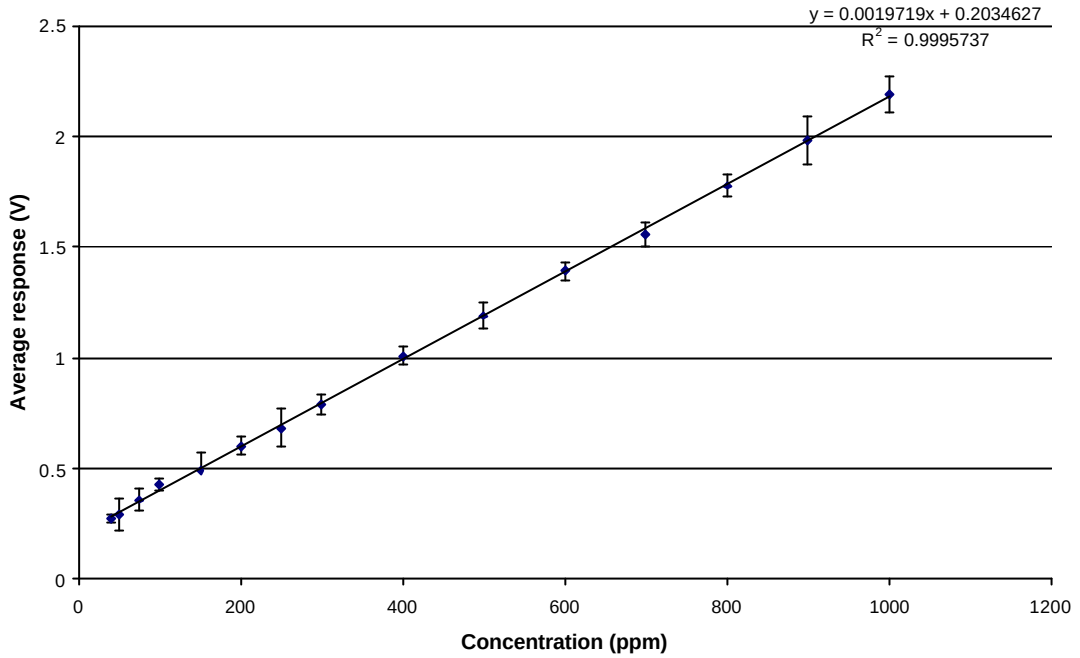


**Figure 7.3**: Calibration graph of nitrous oxide standards with 30x amplifier.

The limit of quantitation is calculated to be 0.26138 *V* which corresponds to a concentration of 29.37 *ppm*. The detection limit is calculated to be 0.22084 *V* corresponding to a concentration of 8.81 *ppm*. A linear relationship with an $R^2$ of 0.999 is observed over the 40 ppm to 1,000 ppm operating range. The error bars shown in figure 7.3 illustrate one standard deviation error calculated from the original data for each standard.

The employment of a 30x amplifier lowered the limit of quantitation by 71.54 *ppm*, and lowered the detection limit of the instrument by 21.46 *ppm*. Inclusion of an amplifier with a higher gain should result in lower detection limits although amplification of the noise eventually limits the advantages to be attained by increasing amplifier gain.

### 7.3.2 Carbon Dioxide

Carbon dioxide standards were measured with the 30x amplifier connected. The calibration graph for carbon dioxide is shown in figure 7.4.

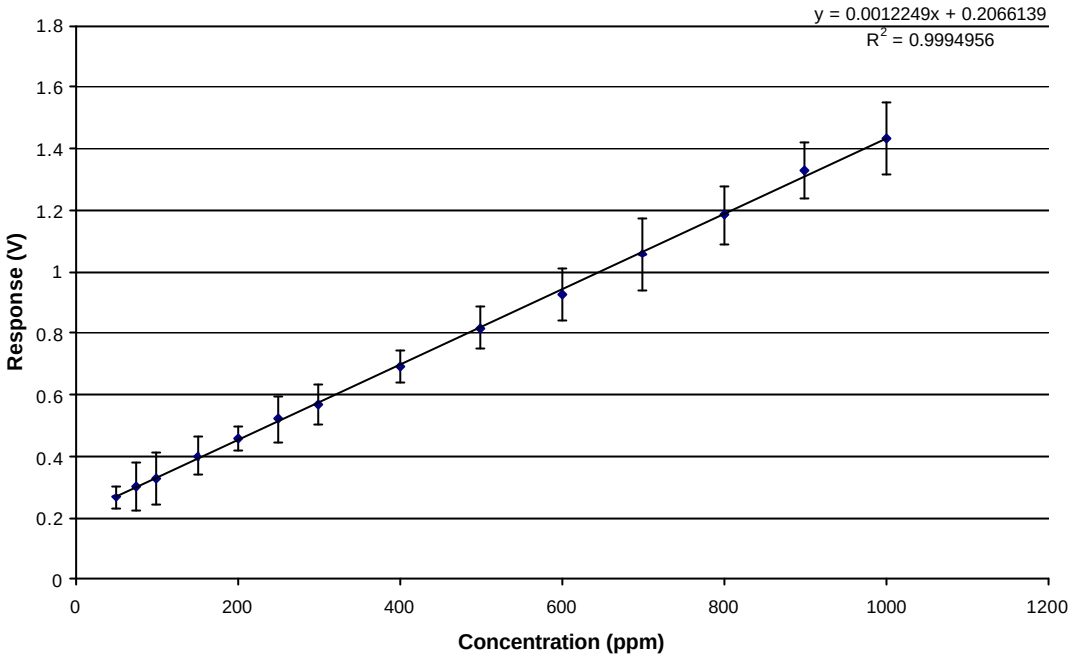


**Figure 7.4**: Calibration graph of carbon dioxide standards with the 30x amplifier.

The limit of quantitation is calculated to be 0.25023 *V* which corresponds to a concentration of 34.46 *ppm*. The detection limit is calculated to be 0.22072 *V* corresponding to a concentration of 10.33 *ppm*. A linear relationship with an $R^2$ of 0.999 is observed. The error bars shown in figure 7.4 illustrate one standard deviation error calculated from the original data.

### 7.3.3 Methane

Methane standards were measured with the 30x amplifier connected. The calibration graph for methane is shown in figure 7.5.

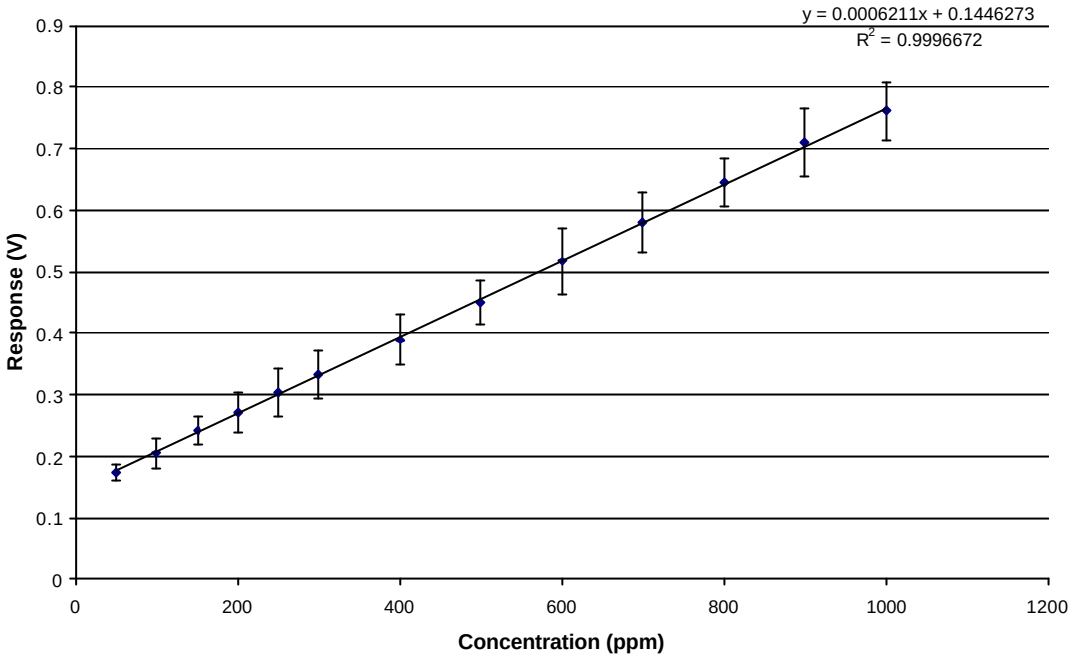


**Figure 7.5**: Calibration graph for methane standards with 30x amplifier.

The limit of quantitation is calculated to be 0.16320 *V* which corresponds to a concentration of 30.59 *ppm*. The detection limit is calculated to be 0.15004 *V* corresponding to a concentration of 9.17 *ppm*. A linear relationship with an $R^2$ of 0.999 is observed. The error bars shown in figure 7.5 illustrate one standard deviation error calculated from the original data.

## 7.4 Air Sample Measurements

To test the concentration of carbon dioxide, methane and nitrous oxide in air, numerous measurements were made. Air was passed through the drying tube with time to allow the removal of water from the air before admitting it to the sample cell. This is an important step, because water has overlapping absorption bands with the three gases.

.

As expected, methane and nitrous oxide resulted in no response because their atmospheric concentrations (1786 *ppb* for methane[11] and 321 *ppb* for nitrous oxide[12])

[11] National Oceanic and Atmospheric Administration. www.noaa.gov
[12] Carbon dioxide Information Analysis Centre. http://cdiac.ornl.gov

are far below the detection limits of the instrument, however, carbon dioxide gave a good response as shown below.

### 7.4.1 Carbon Dioxide

Sixteen air samples were measured for carbon dioxide and their response and corresponding concentration are shown in table 7.1.

| Run | Response (V) | Concentration (ppm) |
|---|---|---|
| 1 | 0.7516 | 378.00 |
| 2 | 0.7605 | 385.30 |
| 3 | 0.7734 | 395.81 |
| 4 | 0.7656 | 389.45 |
| 5 | 0.7692 | 392.39 |
| 6 | 0.7522 | 378.45 |
| 7 | 0.7581 | 383.29 |
| 8 | 0.7451 | 372.70 |
| 9 | 0.7484 | 375.35 |
| 10 | 0.7493 | 376.09 |
| 11 | 0.7713 | 394.11 |
| 12 | 0.7408 | 369.17 |
| 13 | 0.7707 | 393.58 |
| 14 | 0.7363 | 365.52 |
| 15 | 0.7478 | 374.93 |
| 16 | 0.7664 | 390.11 |

**Table 7.1**: Carbon dioxide concentrations in dried laboratory air measurements.

The mean carbon dioxide concentration was calculated to be 382 *ppm* with a standard deviation of 10 *ppm*. This value compares well to current carbon dioxide concentrations of 382.4 *ppm*[13]. A standard deviation of 10 *ppm* shows the instrument has a relatively good precision, however, side-by-side measurements were not taken with a commercial instrument and so the accuracy of the instrument can only be judged against the internationally measured and globally accepted values. In this regard the instrument performs very well and the next logical step would be to design changes aimed at lowering the detection limit.

[13] National Oceanic and Atmospheric Administration. www.noaa.gov

## Chapter VIII

# Conclusion and Future Work

A non-dispersive infrared spectrometer constructed for an M.Sc. project in 2004 has been improved and tested. The final cost of the instrument was US$3,500, making it an affordable gas measurement instrument for today's standards. The instrument was tested to measure laboratory prepared carbon dioxide samples down to 34 *ppm*, nitrous oxide samples down to 29 *ppm*, and methane samples down to 30 *ppm*. In it's development form, the instrument is larger than necessary in order to facilitate design changes but is still relatively portable and can be moved around the laboratory if placed on a trolley. However, the power consumption is too high for the instrument to be field usable without the use of a generator to supply the IR sources. The instrument would be suited for monitoring greenhouse gases in agricultural applications, but is not yet suitable for trace gas measurement. The addition of a beam chopper and lock-in amplifier improved the response and the sensitivity from the inherited instrument, however, these results did not surpass the results obtained from the original instrument constructed in 2004. It has, however, been extended to measure both methane and nitrous oxide as well as carbon dioxide originally used to test the prototype.

A number of major problems were encountered during this research including an unstable baseline due to the differential heating of the glass detector cells. This problem was solved by employing a cooling system which kept the glass cells at a

constant 17°C. However, the requirement for a mains water supply and power supply could be removed by replacing the glass detector cells with double glazed glass cells with a vacuum in the gap, or even ceramic or metallic gas cells. Further improvements could include the addition of infrared laser sources which would reduce the power consumption and remove the requirement for cooling fans however this would only be suitable for single gas analysis. The reference and sample cells could be replaced with multi-pass cells, compacting the instrument and making it more portable. An amplifier with a 30x gain improved the sensitivity of the instrument, therefore the inclusion of an amplifier with a higher gain may increase the sensitivity of the instrument and result in lower detection limits.

The instrument has the potential to be used in a wide range of applications, however, the addition of the beam chopper and lock-in amplifier had little effect on the sensitivity of the instrument, while increasing the cost of the instrument and decreasing its portability. Further improvements to achieve increased portability and versatility will significantly increase the cost of the instrument.

# References


Amato 2002 — F.D. Amato, M. De Rosa. *Optics and lasers in engineering*. 37: 533 – 551; 2002.

Atkins 2006 — P. Atkins, J. de Paula. *Atkins physical chemistry, eighth edition*. Oxford university press, New York, 2006.

Bandstra 2006 — L. Bandstra, B. Hales, T. Takahashi. *Marine Chemistry*. 100: 24 – 38; 2006.

Baren 2004 — R. Baren, M. Parrish, K. Shafer, C. Harward, Q. Shi, D. Nelson, J. McManus, M. Zahniser. *Spectrochimica Acta Part A*. 60: 3437 – 3447: 2004.

Bernstein 2008 — J. A. Bernstein, N. Alexis, H. Bacchus, L. L. Bernstein, P. Fitz, E. Horner, N. Li, S. Mason, A. Nel, J. Oullette, K. Reijula, T. Reponen, J. Seltzer, A. Smith, S. M. Tarlo. *Journal of Allergy and Clinical Immunology*. 121: 585 – 591; 2008

Bhoga 2007 — S. S. Bhoga. K. Singh. *Ionics*. 13: 417 – 427: 2007.

Buchwitz 2000 — M. Buchwitz, V. V. Rozanov, J. P. Burrows. *Journal of geophysical research*. 105: 15,231 – 15,245; 2000.

Cambell 1997 — M. Cambell. *Sensor systems for environmental monitoring. Volume two*. Blackie Academic and Professional, United Kingdom; 1997.

Cazes 2005 J. Cazes. *Analytical instrumentation handbook, third edition*. Marcel Dekker Inc, New York, 2005.

Clarke 1997 A. G. Clarke. *Industrial air pollution monitoring – Environmental management series 8*. Chapman and Hall, London; 1997.

Clerbaux 2003 C. Clerbaux, J. Hadji-Lazaro, S. Turquety, G. Megie, P. Coheur. *Atmospheric Chemistry and Physics*. 3: 1495 – 1508; 2003.

Comini 2006 E. Comini. *Analytica Chimica Acta.* 568: 28 – 40; 2006.

de Castro 1999 A. J. de Castro, J. Meneses, S. Briz, F. Lopez. *Review of Scientific instruments.* 70: 3156 – 3159: 1999.

Down 2005 R. D. Down, J. H. Lehr. *Environmental instrumentation and analysis handbook*. John Wiley and sons Inc, New Jersey; 2005.

Ewing 1997 G.W. Ewing. *Analytical instrumentation handbook, second edition*. Marcel Dekker Inc, New York; 1997.

Fergus 2007 J. W. Fergus. *Sensors and Actuators B.* 122: 683 – 693: 2007.

Gagliardi 2002 G. Gagliardi, L. Gianfrani. *Optics and lasers in engineering*. 37: 509 – 520; 2002.

Garcia 2004 M. L. Garcia, M. Masson. *Environmental Geology*. 46: 1059 – 1063; 2004.

Garzon 2000 F. H. Garzon, R. Mukundan, E. L. Brosha. *Solid State Ionics*. 136 – 137: 633 – 638; 2000.

Gopel 2000 W. Gopel, G. Reinhardt, M. Rosch. *Solid State Ionics*. 136 – 137: 519 – 531; 2000.

Griffith 2002 D. W. T. Griffith, R. Leuning, O. T. Denmead, I. M. Jamie. *Atmospheric Environment*. 36: 1833 – 1842; 2002.

Heard 2006 D.E. Heard. *Analytical techniques for atmospheric measurement*. Blackwell publishing, Oxford; 2006.

Hiyama 1999 T. Hiyama. *Analytica Chimica Acta.* 402: 297 – 302; 1999.

Kalvoda 1975 R. Kalvoda. *Operational amplifiers in chemical instrumentation*. Ellis Horwood Limited, England; 1975.

Kaltin 2005 S. Katin, C. Haraldsson, L. Anderson. *Marine Chemistry*. 96: 53 – 60; 2005.

Kendall 1966 D. Kendall. *Applied infrared spectroscopy*. Reinhold publishing corporation, London; 1966.

Korotcenkov 2007 G. Korotcenkov. *Materials Science and Engineering B.* 139: 1 – 23; 2007.

Kubista 2006 J. Kubista, P. Spanel, K. Dryahina, C. Workman, D. Smith. *Rapid Communications in Mass Spectrometry*. 20: 563 – 567; 2006.

McClave 2003 J. T. McClave, T. Sincich. *Statistics, Ninth Edition*. Prentice Hall Inc, United States; 2003.

Mecca 2000 F.J.M. Mecca et. Al. *Sensors and actuators*. 84: 45 – 52; 2000.

Mokhov 2008 I. I. Mokhov, A. V. Eliseev. *Encyclopedia of ecology, global ecology*. 598 – 602; 2008.

Moseley 1987 P. T. Moseley, B. C. Tofield. *Solid state gas sensors*. IOP publishing Ltd, Bristol; 1987.

Myhre 2000 G. Myhre, A. Myhre, F. Stordal. *Atmospheric Environment*. 35: 2361 – 2373; 2001.

O'Neill 1998 P. O'Neill. *Environmental Chemistry, third edition*. Blackie Academic and Professional, London; 1998.

Raj 2006 E. S. Raj, K. F. E. Pratt, S. J. Skinner, I. P. Parkin, J. A. Kilner. *Chemical Materials*. 18: 3351 – 3355; 2006.

Saggar 2007 S. Saggar, D. L. Giltrap, C. Li, K. R. Tate. *Agriculture, Ecosystems and Environment*. 119: 205 – 216; 2007.

Simpson 2004 T. J. Simpson. *Development of an affordable, portable and versatile infrared gas analyser*. University of Canterbury Thesis; 2004.

Skoog 1998 D. Skoog, F. Holler, T. Nieman. *Principles of instrumental analysis, fifth edition*. Thomson Learning, United States; 1998.

Smith 1996 B. Smith. *Fundamentals of Fourier transform infrared spectroscopy*. CRC Press, Inc, Florida; 1996.

Smith 2004 D. Smith, P. Spanel, D. Dabill, J. Cocker, B. Rajan. *Rapid Communications in Mass Spectrometry*. 18: 2830 – 2838; 2004.

Smith 2005 D. Smith, P. Spanel. Mass Spectrometry Reveiws. 24: 661 – 700; 2005.

Somesfalean 2005 G. Somesfalean, J. Alnis, U. Gustafsson, H. Edner, S. Svanberg. *Applied optics*. 44 (24); 2005.

Stauffer 2002 B. Stauffer, J. Fluckiger, E. Monnin, J. Chwander, J. Barnola, J. Chappellaz. *International Glaciological Society.* 35: 202 – 208; 2002.

Theocharous 2007 E. Theocharous. *Infrared physics and technology*. 50: 63 – 69; 2007.

VanLoon 2000 G. W. VanLoon, S. J. Duffy. *Environmental chemistry*. Oxford University Press Inc, New York; 2000.

Vogel 1996 A. I. Vogel, G. Svehla. *Vogel's qualitative inorganic analysis, 7th edition*. Longman Scientific and Technical, New York; 1996.

Willard 1988 H. H. Willard, L. L. Merritt Jr, J. A. Dean, F. A. Settle Jr. *Instrumental methods of analysis, seventh edition*. Wadsworth publishing company, California; 1988.

Wuebbles 2002 D. J. Wuebbles, k. Hayhoe. *Earth-Science Reviews.* 57: 177 – 210; 2002.

# Appendix A

# Operating Procedures

## A.1 Introduction

This appendix contains the operating procedures for the preparation of standards and the operation of the instrument. These operating procedures should be followed for any subsequent use of the instrument. Refer to figure A.1 for references to the gas delivery line.

## A.2 Preparing the Instrument

### A.2.1 Filling Reference Cell

1. Connect the make-up gas cylinder (dry nitrogen or argon) to the gas line. With the regulator valve (low pressure side) closed, open the cylinder valve to register a pressure of approximately 1000 *Torr*.
2. With valves 1, 4, 7, 10, 11 and 12 closed, evacuate the gas delivery line and gas tank 2.
3. Close valve 9.
4. Open the regulator valve until the pressure reaches 1000 *Torr*. Close the regulator valve, and valves 5 and 2.
5. Open valve 9 and evacuate the gas line.
6. Close the main valve on the make-up gas cylinder and disconnect from the gas line.

7. Remove the reference cell from the instrument and attach one of its ¼" gas inlet ports to valve 5 using a teflon ferrule. Open the Young's valve attached to the port keeping the second port closed.
8. Open valve 5 and evacuate the reference cell.
9. Close valve 9.
10. Open valve 2 until the pressure in the gas line and reference cell equals 1 atm.
11. Close the Young's valve on the reference cell and valve 5.
12. Remove the reference cell from the gas delivery line and place back in the instrument.
13. Open valve 9 to evacuate the gas line.
14. Repeat steps 1-13 each time the gas required to be measured is changed.

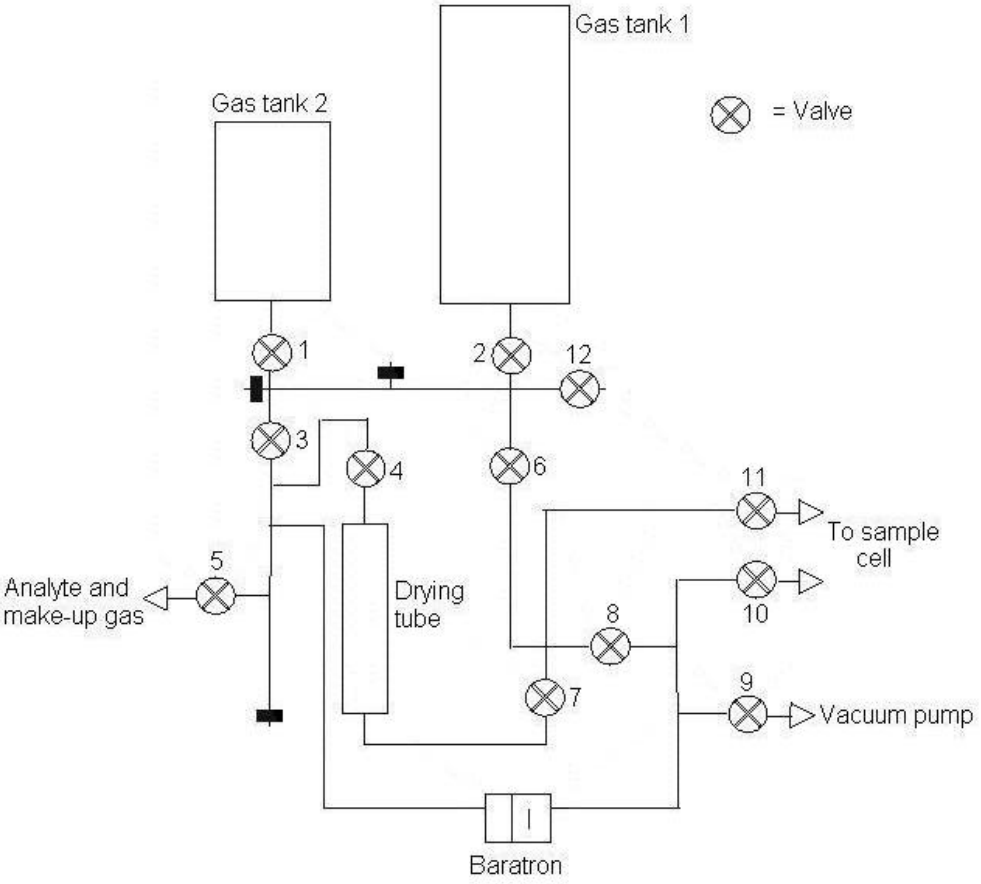


**Figure A.1**: Gas delivery line.

### A.2.2 Filling the Detector Cells

1. Close all valves in the gas line.
2. Connect analyte gas cylinder to one swagelock valve on the detector unit and connect the other swagelock valve to the connection at valve 5 on the gas line.
3. Open main valve on analyte gas cylinder and increase regulator pressure to approximately 1000 *Torr* and keep regulator valve closed.
4. Open valves 3, 5, 6, 8 and 9. Also open both swagelock valves on the detector and the valve separating each side. Pump down the gas line and the detector cells.
5. Close valve 9.
6. Open regulator valve until the pressure reaches approximately 800 *Torr*.
7. Close the regulator valve, both swagelock valves on the detector, and valve 5.
8. Close main valve on the analyte gas cylinder and disconnect from the detector cells.
9. Disconnect connection from detector cells and gas line.
10. Open valve 9. Pump down gas line.
11. Close valve 9.

### A.2.3 Preparation of the Instrument

1. With valves 1, 2, 4, 5 and 12 closed, open valves 3, 6, 7, 8, 9, 10 and 11 and evacuate the gas line and sample cell.
2. Switch on infrared sources, beam chopper and lock-in amplifier.
3. Set the chopping speed to 1.5 Hz and the phase on the lock-in amplifier to 62 degrees.
4. Turn on tap to allow water to flow through the cooling sleeve around the detector.

### A.2.4 Computer

1. Open the data collection program located on the desktop of the computer.
2. Set the stored data points to 4096.
3. Set the refresh rate to 10 samples per second.
4. Click the start button to begin.

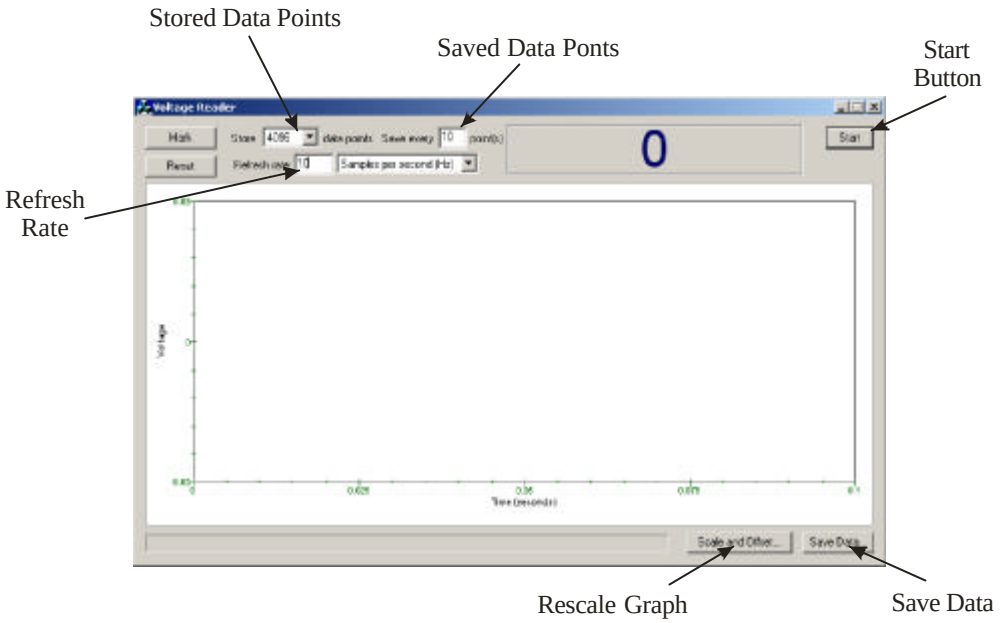


**Figure A.2**: Computer interface control functions [Simpson 2004].

## A.3 Instrument Calibration

Before sample analysis is carried out, gas mixtures of known analyte composition in argon or dry nitrogen must be prepared and a calibration graph for the analyte measured.

### A.3.1 Standard Gas Mixture Preparation

| Required standard ppm | Initial pressure of analyte in Tank 1 | Pressure 1 | Pressure 2 |
|---|---|---|---|
| 10 *ppm* | 100 *Torr* | 10 *Torr* | 10 *Torr* |
| 50 *ppm* | 500 *Torr* | | |
| 200 *ppm* | 200 *Torr* | 10 *Torr* | 100 *Torr* |
| 600 *ppm* | 600 *Torr* | | |
| 3,000 *ppm* | 300 *Torr* | 10 *Torr* | |
| 7,000 *ppm* | 700 *Torr* | | |
| 40,000 *ppm* | 400 *Torr* | 100 *Torr* | |
| 80,000 *ppm* | 800 *Torr* | | |

**Table A.1**: Table for standard preparation.

1. With all valves closed turn on the gas inlet pump, open valves 2, 3, 6, 8 and 9 and evacuate the gas line and gas tank 1 until pressure reaches 0 *Torr*.

2. Connect analyte gas cylinder and open main valve. With the regulator valve closed increase regulator pressure to approximately 1000 *Torr*
3. Open valve 5 and pump down the line to the gas cylinder regulator valve.
4. Close valve 9.
5. Open regulator valve and increase pressure in the gas line until it reaches the *initial analyte pressure* in table A.1. Close regulator valve, and main valve.
6. Close valves 2 and 5.
7. Open valve 9 and pump down the gas line to 0 *Torr*.
8. Disconnect analyte gas cylinder and connect make-up gas cylinder. Open main cylinder valve and with low pressure valve closed increase the regulator pressure to slightly above 1000 *Torr*.
9. Open valve 5 and evacuate the line to the gas cylinder regulator valve.
10. Close valve 9.
11. Open regulator valve and increase pressure in the gas line to 1000 *Torr*. Close regulator valve.
12. Open valve 2. Pressure will drop.
13. Open regulator valve and increase pressure in the gas line and gas tank 1 to 1000 *Torr*.
14. Close valve 2. *Gas tank 1 contains mixture 1*.
15. Open valve 9 and pump down the gas line to 0 *Torr*.
16. Close valve 9.
17. Open valve 2. Pressure will increase to approximately 950 *Torr*.
18. Open valve 9 slowly and pump down mixture to *pressure 1* specified in table A.1.
19. Close valve 9 and 2.
20. Open valve 9 and pump down the gas line to 0 *Torr*.
21. Repeat steps 11 to 16 for all standards. *Gas tank 1 contains mixture 2*.
22. For low concentration standards repeat steps 17 to 21, except in step 18 pump down the mixture to *pressure 2* specified in table A.2.
23. Repeat steps 16 to 21 for other standards as required..

### A.3.2 Measurements for Obtaining a Calibration Curve

1. With valves 1, 2, 4, 5, 7 and 12 closed, evacuate the gas line and sample cell.
2. Close the separating valve on the instrument and remove the blocking plate in front of the infrared sources.
3. Open the computer program and click “Save Data”.

4. Enter the name of the file and click “Save”.
5. Measure the baseline for 10 seconds.
6. Close valves 8 and 10. Open valve 2 until the pressure in the gas line and sample cell reaches 1 *atm.* Note the data time at which the sample was admitted to the instrument.
7. Measure the sample peak for 20 seconds.
8. Close valve 11 and immediately open valve 10 noting the data time at which the sample was removed from the instrument.
9. Measure the baseline for a further 10 seconds.
10. Click the “Stop Saving” button on the computer program.
11. Open the separating valve and place the blocking plate in front of the infrared sources.
12. Open valve 8 and 11 to evacuate the gas line.
13. Repeat steps 1-12 for each standard measurement.

### A.3.3 Measurement of a Sample

1. With valves 1, 2, 5 and 12 closed, evacuate the gas line and the sample cell. Repeat steps 2-5 in section A.3.2.
2. Close valves 6, 8, and 10 and open valve 12 to allow the air sample to flow through the drying tube into the sample cell. Note the data time the sample is admitted into the instrument. Close valve 12.
3. Repeat steps 7-11 in section A.3.2.
4. Open valves 6, 8 and 10 to evacuate the gas line.
5. Repeat steps 1-5 for each sample measurement.

## A.4 Data Analysis

### A.4.1 Obtaining Peak Value

1. Open Microsoft® Excel with a new worksheet.
2. In the data menu select “Import External Data” and then click on “Import Data”.
3. Select the file and click “open”.
4. In the text import wizard click on fixed width and then click “next”.
5. Click between the two columns of data in the text import wizard so an arrow is produced separating the two columns. Click “Finished”.

6. Select the cell you want the first data point to be entered into and click “OK”. The data will form two columns. The left column has the time values and the right column has the corresponding Baratron output voltage values.
7. From the first point select all the points from both columns up to five seconds before the time of admitting the sample.
8. Hold down the “Ctrl” key and select all the points from both columns ten seconds after the sample was removed.
9. In the “Insert” menu select the “chart” option.
10. The “Chart wizard” will open. Select the XY (Scatter) chart and the individual points chart. Select “Next” and “Finish”.
11. The graph of the baseline points will appear in the worksheet. In the “Chart” menu select the “Add trendline” option.
12. Select “Linear” trendline and then select the “options” tab.
13. Select “Display equation on chart” and “Display R-squared value on chart” options. Click “OK”.
14. The trendline for the data will appear on the chart along with the $R^2$ value and the equation for the line. Select the equation and in the “Format” menu select “Select Data Labels”. Select the “Number” tab and chose the “Scientific” category. Change the number or decimal places to at least 5 and click “OK”.
15. Select the equation of the line and copy it into the same row as the first data point in the worksheet. Rearrange the equation to equal zero and then replace the “x” value in the equation for the cell in the same row that has the time, and the “y” value in the equation for the cell in the same row that has the voltage.

    For example: $y = 3.7475758E-02x + 1.6948793$

    will become: $y - (3.7475758E-02x + 1.6948793) = 0$

    should be entered: $= B1 - (3.7475758E-02 * A1 + 1.6948793)$

16. Select the cell the value has been calculated in and “Fill Down” for all data values. While these values are select the “Insert” menu and select “Chart”.
17. The “Chart Wizard” will then open. Select the XY (Scatter) chart and the individual points chart. Select “Next” and “Finish”. This chart generated is the direct response curve with the baseline running through zero.

18. Select all the peak data values of the direct response curve to obtain the average of these using, for example, the calculation: =AVERAGE(C55:C68). This is the value of the sample peak.
19. Repeat steps 2-18 for all samples.

### A.4.2 Establishing a Calibration Curve

1. Carry out all the steps in section A.3.2 and A.4.1 for all calibration standards.
2. In the worksheet arrange the concentration of the calibration standard in one column and the corresponding response peak value in the next column.
3. Select the two columns and in the "Insert" menu select "Chart".
4. In the "Chart Wizard" elect the XY (Scatter) chart and the individual points chart. Select "Next" and "Finish".
5. The calibration graph will then appear in the worksheet. In the "Chart" menu select "Add Trendline".
6. Select "Linear" trendline and then select the "Options" tab.
7. Select "Display equation on chart" and "Display R-squared value on chart" options. Click "OK".
8. The trendline for the data will appear on the chart along with the $R^2$ value and the equation for the line. Select the equation and in the "Format" menu select "Select Data Labels". Select the "Number" tab and chose the "Scientific" category. Change the number or decimal places to at least 7 and click "OK".

### A.4.3 Determining the Concentration of a Sample

1. Carry out all the steps in section A.4.1.
2. Substitute this value as the "y" value in the equation generated from the calibration curve and solve for "x".
3. The value for x is the concentration for the sample.

## Appendix B

# Statistical Analysis

## B.1 Linear Regression

Linear least squares regression is used to determine the "best fit" relationship between two sets of data (x and y) for establishing a calibration curve. This is achieved by finding the relationship between x and y that gives the sum of squared errors (SSE) at a minimum.

The fitted line can be written as:

$$y = mx + c \qquad \text{B.1}$$

Where $y$ = the detector response in volts,
$m$ = slope of the graph,
$x$ = the standard concentration,
$c$ = the y-intercept of the line.

A residual is the vertical deviation of each point from the straight line on the calibration graph. These are defined as: sum of squares of deviations for x ($SS_{xx}$); sum of squares of deviations for y ($SS_{yy}$); and sum of squares of deviations for x and y ($SS_{xy}$).

$$SS_{xx} = \Sigma x_i^2 - \frac{(\Sigma x_i)^2}{n} \quad \text{B.2}$$

$$SS_{yy} = \Sigma y_i^2 - \frac{(\Sigma y_i)^2}{n} \quad \text{B.3}$$

$$SS_{xy} = \Sigma x_i y_i - \frac{\Sigma x_i y_i}{n} \quad \text{B.4}$$

Where $x_i$ = coordinates for individual data points x,

$y_i$ = coordinates for individual data points y,

$n$ = number of data points used in the calibration graph.

These quantities can be used to calculate the slope and intercept of the line for the calibration graph as well as the standard deviations of these parameters, as shown below.

Slope of the calibration graph, m:

$$m = \frac{SS_{xy}}{SS_{xx}} \quad \text{B.5}$$

Intercept of the calibration graph, c:

$$c = \bar{y} - m\bar{x} \quad \text{B.6}$$

Where $\bar{y}$ = average value for y,

$\bar{x}$ = average value for x.

Standard deviation about regression, $S_r$:

$$S_r = \sqrt{\frac{SS_{yy} - m^2 SS_{xx}}{n-2}} \qquad \text{B.7}$$

Standard deviation of the slope, $S_m$:

$$S_m = \frac{S_r}{\sqrt{SS_{xx}}} \qquad \text{B.8}$$

Standard deviation of the intercept, $S_c$:

$$S_c = S_r \sqrt{\frac{1}{n - \frac{(\Sigma x_i)^2}{\Sigma x_i^2}}} \qquad \text{B.9}$$

When measuring a sample these parameters can then be used to determine the standard deviation for the results obtained from the calibration graph.

Standard deviation for analytical results, S:

$$S = \frac{S_r}{m} \sqrt{\frac{1}{N} + \frac{1}{n} + \frac{(\overline{y_s} - \overline{y})^2}{m^2 SS_{xx}}} \qquad \text{B.10}$$

Where $\overline{y_s}$ = average value for y in the sample,

$N$ = number of replicate analyses of the sample

The coefficient of determination, $R^2$, is a measure of the linearity of the relationship between the two variables x and y. The value is in the range from 0 to 1. The stronger the linear relationship is between the variables the closer the $R^2$ value will be to 1. The $R^2$ value can be determined from the following equation:

$$R^2 = 1 - \frac{\Sigma(y_i - \bar{y})^2}{(\Sigma y_i^2) - \frac{(y_i)^2}{n}} \qquad \text{B.11}$$

## B.2 Accuracy and Precision

All measurements contain errors and are only approximations of the "true" value. Accuracy describes how close the measured value is to the "true" value. This can be expresses as either relative error or absolute error shown below.

Absolute error, $E_a$:

$$E_a = \bar{x} - x_t \qquad \text{B.12}$$

Where $E_a$ = absolute error,

$\bar{x}$ = average of data set x,

$x_t$ = an acceptable value for the quantity being measured.

Relative error, Er:

$$E_r = \frac{\bar{x} - x_t}{x_t} \times 100 \qquad \text{B.13}$$

Precision is a measure of the reproducibility of the results. This shows the relative agreement between numerous replicated measurements. Precision is illustrated by calculating the standard deviation (S) and variance ($S^2$) of the replicated measurements, shown below.

Standard deviation, S:

$$S = \sqrt{\frac{\Sigma(x_i - \bar{x})^2}{n-1}} \qquad \text{B.14}$$

## B.3 Detection Limit, Limit of Quantitation and Limit of Linearity

The detection limit (DL) is the minimum concentration that can be detected at a known confidence level [Skoog 1998]. It is calculated using the following equation,

$$DL = b + 3S_b \qquad \text{B.15}$$

Where $DL$ = Detection limit,

$b$ = blank measurement,

$S_b$ = Standard deviation of the blank signal.

The standard deviation of the blank measurement generally requires at least twenty measurements. The detection limit can also be determined when using linear regression for the calibration curve [Simpson 2004] using equation B.16,

$$DL = c + 3S_c \qquad \text{B.16}$$

Where $c$ = Intercept of the line on the calibration curve,

$S_c$ = Standard deviation of the intercept.

This can also be expressed in terms of the slope of the calibration curve as shown below.

$$DL = \frac{3S_c}{m} \qquad \text{B.17}$$

The dynamic range of an analytical method extends from the limit of quantitation up to the limit of linearity [Skoog 1998]. The limit of quantitation (LOQ) is the lowest concentration for which a quantitative measurement can be made while obtaining high precision. The limit of quantitation is expressed below.

$$LOQ = \frac{10S_c}{m} \qquad \text{B.18}$$

The limit of linearity is the point where the calibration curve departs from linearity. This value is determined from analysis of the calibration graph as shown in figure B.1.

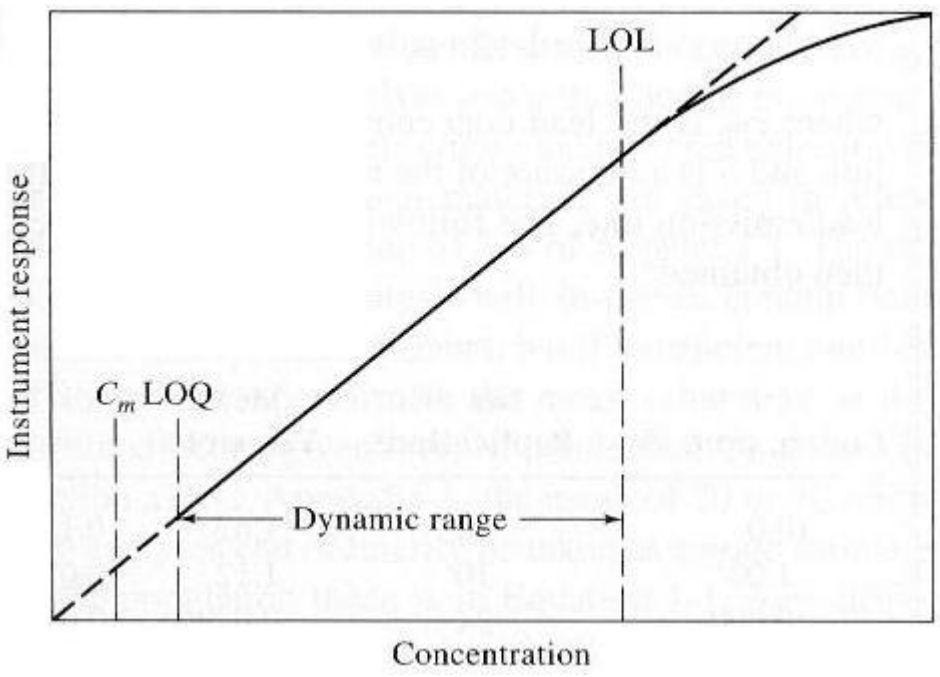


**Figure B.1**: Dynamic range for an analytical instrument [Skoog 1998].